

whether EAAT2 detergent insolubility is elevated in AD, we developed 2 independent EAAT2 ELISAs. This approach was adopted to facilitate quantification of the relatively large number of samples to be tested (102 cortex and 53 hippocampus samples were measured in triplicate).

Specificity of EAAT2 Detection

The AB12 is a polyclonal antibody that recognizes an amino-terminus epitope common to all EAAT2/GLT-1 isoforms; GLT-1A is a polyclonal antibody that recognizes the C-terminal domain of the dominant EAAT2 isoform expressed in the brain (20). These antibodies were tested under a variety of conditions using brain tissue from GLT-1 wild-type and GLT-1 knockout (KO) mice. Figure 2 shows that AB12 and GLT-1A selectively recognized EAAT2/GLT-1 by ELISA (Fig. 2A). In addition, we verified that EAAT2/GLT-1 levels measured by these ELISAs increased as a linear function of protein assayed (linear regression for AB12 ELISA: $r^2 = 0.8799$, $F_{1,23} = 168.6$, $p < 0.0001$; GLT-1A ELISA: $r^2 = 0.9567$, $F_{1,23} = 507.8$, $p < 0.00001$). The AB12 and GLT-

1A also detected GLT-1 by immunohistochemistry (Fig. 2B) and recognized Triton X-100-soluble GLT-1 via Western blots (Fig. 2C) from GLT-1 wild-type, but not GLT-1 KO, mice. These data prove that AB12 and GLT-1A specifically recognize EAAT2.

Detergent-Insoluble EAAT2 Aberrantly Accumulates in AD

Frontal cortex and hippocampus tissue samples were serially extracted $\times 3$ with Triton X-100 to remove detergent-soluble proteins, and residual detergent-insoluble proteins were then solubilized with formic acid. Neutralized formic acid-extracted proteins and the first Triton X-100-soluble fraction were analyzed by ELISAs to determine the relative levels of detergent-insoluble and detergent-soluble EAAT2.

In hippocampus samples, detergent-insoluble EAAT2 levels were elevated in AD patients compared with normal controls and PD patients, whereas detergent-insoluble EAAT2 levels in CDR = 0.5 patients were intermediately elevated between the controls and later-stage AD patients (Figs. 3A, B).

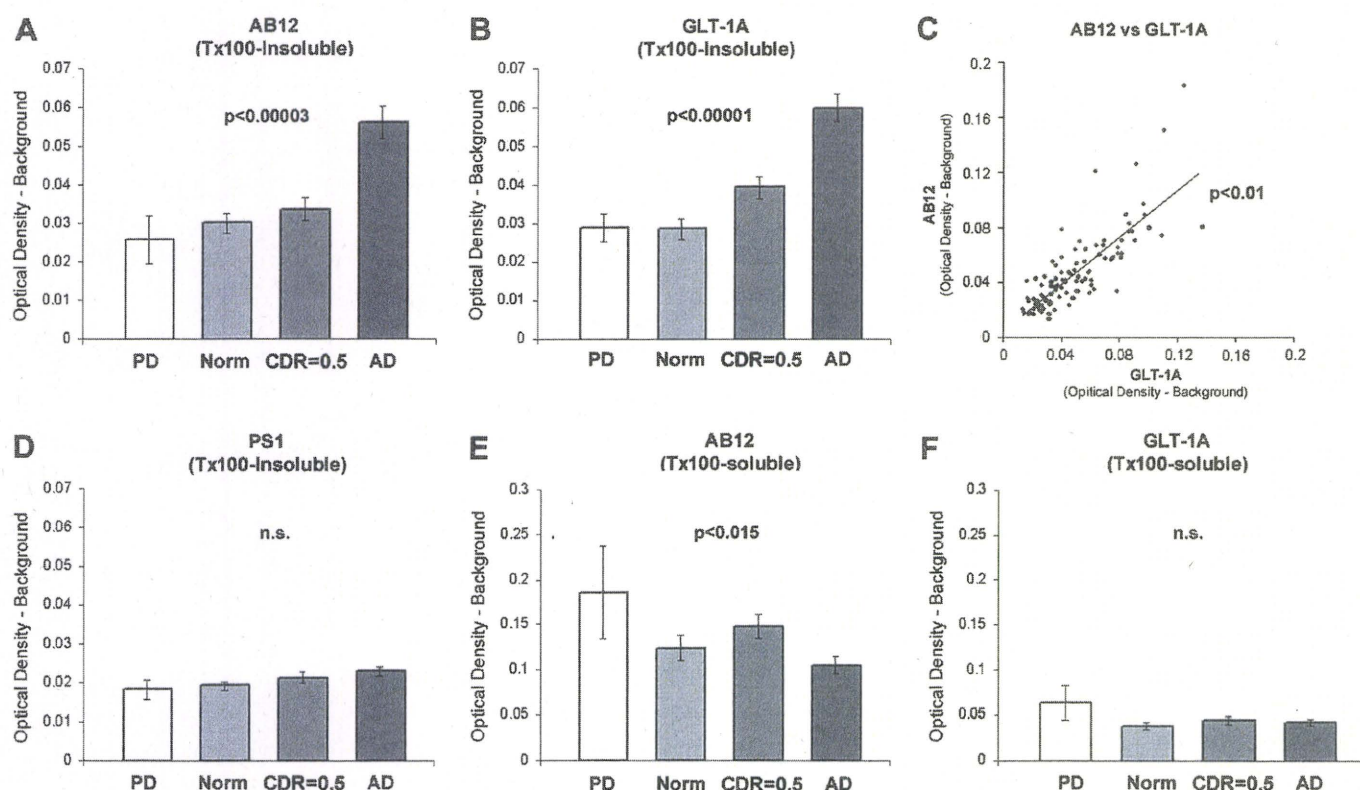
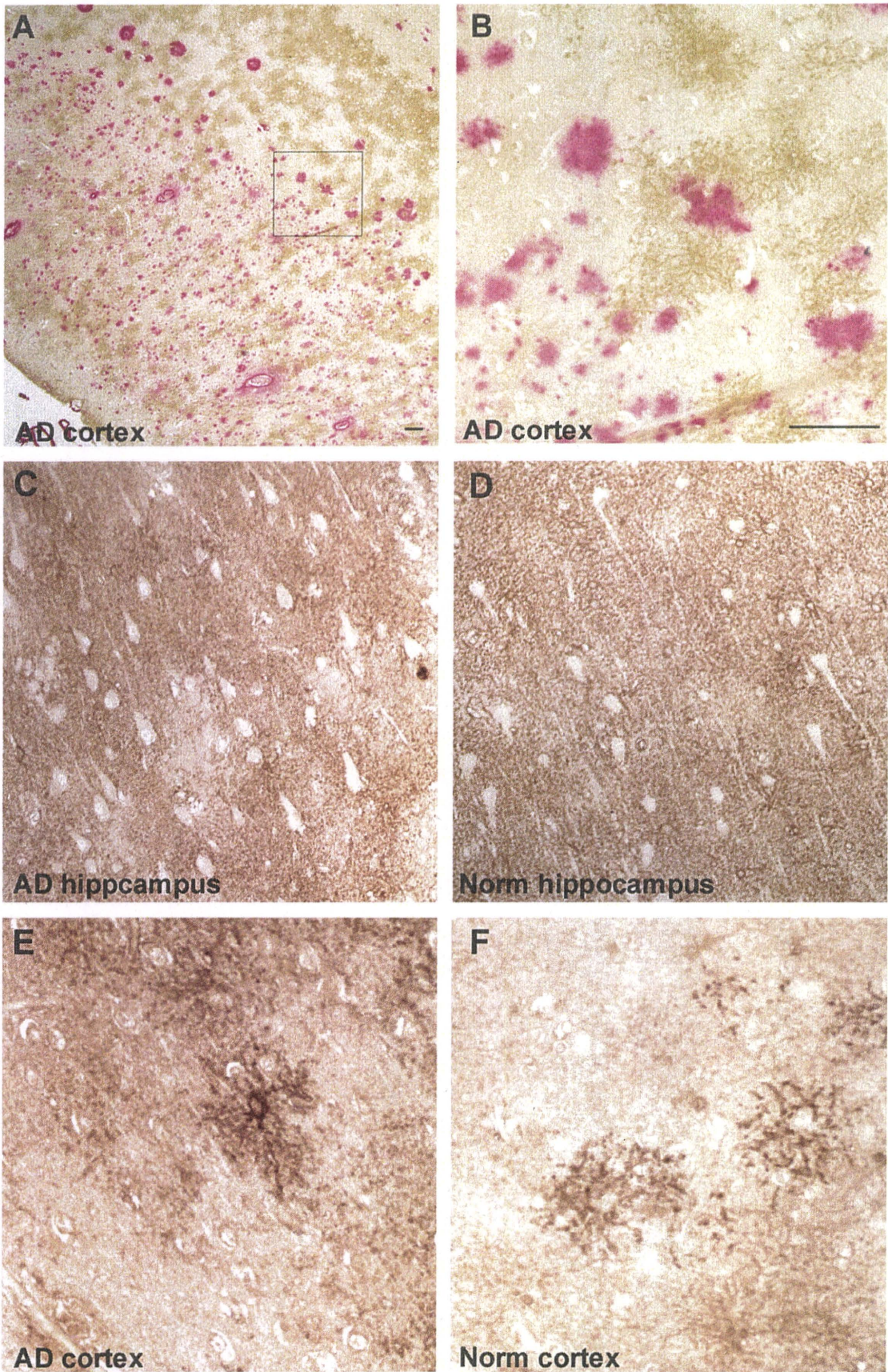


FIGURE 4. Detergent-insoluble excitatory amino acid transporter 2 (EAAT2) levels were increased in the frontal cortex of patients with Alzheimer disease (AD) pathology. **(A)** Total Triton X-100-insoluble proteins from Parkinson disease (PD, $n = 4$), normal control (Norm, $n = 20$), mild cognitive impairment ($n = 23$), and later-stage AD ($n = 55$) patients were solubilized with formic acid and analyzed by AB12 ELISA to quantify detergent-insoluble EAAT2 levels. **(B)** Total Triton X-100-insoluble EAAT2 levels were measured by GLT-1A ELISAs as in **(A)**. **(C)** Scatter plot shows a correlation between insoluble EAAT2 levels measured by AB12 and GLT-1A ELISAs for all subjects ($n = 102$). The p value indicates statistical significance determined by Pearson correlation. **(D)** Total Triton X-100-insoluble levels of presenilin-1 (PS1) were measured in the same samples as shown **(A)** and **(B)**. **(E, F)** Triton X-100-soluble EAAT2 levels from the same samples as in **(A, B, and D)** were measured by AB12 and GLT-1A ELISAs, respectively. The p values in **(A, B, D-F)** indicate results of overall single-factor analysis of variance. CDR, Clinical Dementia Rating; n.s., not significant.



These differences in detergent-insoluble EAAT2 levels among groups detected either with AB12 or GLT-1A ELISA were statistically significant ($F_{3,49} = 7.107$, $p < 0.0005$; $F_{3,49} = 6.733$, $p < 0.0007$, respectively). These data suggest that EAAT2 becomes increasingly detergent-insoluble as AD-related pathology progresses from the less demented state to CDR = 0.5, and then becomes most pronounced by later-stage AD. A contrast analysis tested the prediction that detergent-insoluble EAAT2 levels followed a statistically significant trend where normal = PD < CDR = 0.5 < AD (AB12 $t_{49} = 3.685$, $p < 0.001$; GLT-1A $t_{49} = 3.353$, $p < 0.002$). The scatter plot in Figure 3C shows that detergent-insoluble EAAT2 levels in hippocampus measured by AB12 and GLT-1A ELISAs were positively correlated ($r = 0.820$, $n = 53$, $p < 0.01$), thereby confirming the close correspondence between 2 independent assays that shows that EAAT2 detergent insolubility increases as AD pathology increases.

In marked contrast to these findings, Triton X-100-insoluble PS1 levels (Fig. 3D) in the same samples did not differ among groups ($F_{3,49} = 2.141$, not significant [n.s.]). Presenilin-1 was chosen for comparison because it is localized prominently in astrocytes (26) that express approximately 80% of the EAAT2 in hippocampus and because overall PS1 expression levels are not affected by AD (27). These data argue that the detergent insolubility displayed by EAAT2 was not the result of generalized nonspecific cellular injury. Moreover, PS1 is structurally similar to EAAT2. Each molecule has 8 hydrophobic membrane-spanning domains with the N- and C-terminal domains localized intracellularly (27). Thus, the detergent insolubility profiles of EAAT2 obtained from the identical samples are unlikely to have arisen by nonspecific protein-protein interactions that might have occurred during the extraction process.

We also examined detergent-soluble EAAT2 levels in the same hippocampal samples (Figs. 3E, F). In contrast to the significant trend of increasing EAAT2 detergent insolubility, there was a statistically significant difference among groups in detergent-soluble EAAT2 levels detected by AB12 ELISAs ($F_{3,49} = 3.237$, $p < 0.030$); detergent-soluble EAAT2 levels seemed to decrease with increasing AD pathology. Differences in detergent-soluble EAAT2 levels detected by GLT-1A ELISAs were not statistically significant ($F_{3,49} = 2.468$, n.s.).

Because detergent-soluble EAAT2 levels were comparatively low in AD patients compared with normal controls

whereas the detergent-insoluble EAAT2 levels were markedly elevated in the same samples, it is highly unlikely that the increased detergent-insoluble EAAT2 measured in AD patients could have been caused by incomplete extraction of Triton X-100-soluble EAAT2 or that this reflects nonspecific EAAT2 associations with detergent-insoluble amyloid plaques or NFTs. This conclusion was further supported by the findings that detergent-soluble EAAT2 levels were not significantly correlated with detergent-insoluble A β levels measured by 4G8 ELISAs (AB12 vs A β : $r = -0.167$, $n = 53$, n.s.; GLT-1A vs A β : $r = -0.162$, $n = 53$, n.s.). Similarly, detergent-soluble EAAT2 levels were not correlated with insoluble tau levels measured by tau-2 ELISAs (AB12 vs tau: $r = -0.141$, $n = 53$, n.s.; GLT-1A vs tau: $r = -0.131$, $n = 53$, n.s.). These findings argue against the possibility of nonaggregating EAAT2 in the lysates nonspecifically associated with the insoluble A β or insoluble tau.

As in the hippocampi, Triton X-100-insoluble EAAT2 levels were markedly elevated in AD frontal cortex compared with PD and normal control subjects (Figs. 4A, B). Detergent-insoluble EAAT2 levels measured by GLT-1A ELISAs in CDR = 0.5 subjects again fell between controls and AD levels (Fig. 4B), whereas increased detergent-insoluble EAAT2 levels measured by AB12 ELISAs in CDR = 0.5 cortex were less pronounced (Fig. 4A). These differences in detergent-insoluble EAAT2 levels among groups were significant (AB12 ELISA: $F_{3,98} = 8.743$, $p < 0.00003$; GLT-1A ELISA: $F_{3,98} = 13.375$, $p < 0.00001$). Detergent-insoluble EAAT2 levels in frontal cortex (Figs. 4A, B) followed the predicted trend: controls = PD < CDR = 0.5 < AD, confirmed by statistically significant contrast test outcomes for both AB12 and GLT-1A ELISAs ($t_{98} = 3.100$, $p < 0.002$; $t_{98} = 4.087$, $p < 0.0001$, respectively). Figure 4C shows a significant positive correlation between detergent-insoluble EAAT2 levels measured using AB12 versus GLT-1A ($r = 0.801$, $n = 102$, $p < 0.01$). Triton X-100-insoluble PS1 levels in frontal cortex (Fig. 4D) did not significantly differ among groups ($F_{3,98} = 1.651$, n.s.). In contrast to hippocampus (Figs. 3E, F), detergent-soluble EAAT2 expression levels in the frontal cortex of normal controls, CDR = 0.5, and AD patients (Figs. 4E, F) were similar (AB12 ELISA: $F_{3,98} = 3.669$, $p < 0.015$; GLT-1A ELISA: $F_{3,98} = 1.330$, n.s.). Again, detergent-soluble EAAT2 levels in the frontal cortex did not correlate with the levels of detergent-insoluble A β or tau measured in the same samples (AB12 vs A β : $r = -0.160$, $n = 102$, n.s.; GLT-1A vs A β : $r = -0.008$, $n = 102$, n.s.; AB12 vs tau: $r = -0.105$,

FIGURE 5. Excitatory amino acid transporter 2 (EAAT2) immunohistochemistry (IHC) in Alzheimer disease (AD) and normal controls. **(A)** EAAT2 IHC using AB12 (brown) in AD frontal cortex reveals an irregular patchy astrocyte-like expression pattern that does not correspond with senile plaques immunostained red with the anti-amyloid- β (A β) monoclonal antibody 4G8. **(B)** Higher magnification of the boxed region in **(A)** highlights the lack of correspondence between EAAT2 immunoreactivity and A β deposits. Some plaques appeared to be surrounded by EAAT2 immunoreactivity, whereas other plaques were localized in EAAT2 immunonegative domains. **(C, D)** The EAAT2 was immunostained with AB12 (brown) in the hippocampal CA1 region of an AD **(C)** and a normal control (Norm **[D]**). The EAAT2 expression was primarily densely stained perisynaptic and extrasynaptic EAAT2-positive puncta in the neuropil. **(E)** Apparent astrocyte immunostained with AB12 in AD frontal cortex where proximal and distal glial processes and the cell body display EAAT2 immunoreactivity. Prominent EAAT2 immunostaining in astrocyte-like cell bodies was more readily detected in AD than in controls. **(F)** The AB12-immunostained apparent astrocytes in normal control revealed abundant EAAT2 immunoreactivity in proximal and distal processes, with less prominent cell body staining.

$n = 102$, n.s.; GLT-1A vs tau: $r = -0.049$, $n = 102$, n.s.), thus arguing against the possibility that incomplete extraction or nonspecific EAAT2 protein-protein interactions occurred during tissue processing.

EAAT2 Localization Appears Comparatively Normal in AD

In normal brain tissue, EAAT2 is localized primarily, but not exclusively, in fine astrocytic processes that densely ramify throughout perisynaptic and extrasynaptic domains (28, 29). We performed immunohistochemistry to determine whether aberrant EAAT2 expression was localized near amyloid plaques, in association with NFTs, or aberrantly accumulated in neuronal or astrocytic cell bodies.

Double label immunostaining failed to reveal a consistent morphological association between EAAT2 expression and A β deposits in AD, which argues against the idea that EAAT2 accumulated in association with senile plaques in vivo (Figs. 5A, B). In keeping with the predominantly astrocytic expression pattern characteristic of EAAT2, we found a paucity of EAAT2 immunoreactivity in neuronal cell bodies and dendritic processes in both AD and normal control brains (Figs. 5C, D). The primary morphologically neuron-like EAAT2 expression pattern observed was that associated with apparent neurofibrillary ghost tangles in AD subjects that immunostained weakly for EAAT2 (not shown). Thus, we found limited evidence that EAAT2 was prominently associated with NFTs, a finding consistent with the fact that NFTs are localized primarily in neurons but not in astrocytes in AD (30).

Close inspection of EAAT2 immunostaining revealed that EAAT2 was expressed in distal processes and to a lesser extent in cell bodies, both in AD and control brains. Nonetheless, astrocytes with prominent cell body EAAT2 immunostaining were more readily identified in AD frontal cortex than in normal control cortex (Figs. 5E, F). Despite this potentially interesting nonquantitative distinction between AD and control subjects, the overall immunohistochemical findings suggested that EAAT2 localization was not dramatically altered in AD patients compared with controls.

DISCUSSION

Aberrant EAAT2 Detergent Insolubility Is a Novel Biochemical Lesion in AD

Using 2 independent ELISA systems to measure detergent-insoluble EAAT2, along with corroborating mass spectrometry, we found that detergent-insoluble EAAT2 is aberrantly elevated in AD patient brains compared with controls and intermediately elevated in mildly impaired CDR = 0.5 patients with autopsy-confirmed early AD neuropathology. These data argue that EAAT2 detergent insolubility represents a progressive biochemical lesion of AD. The findings further suggest that EAAT2 belongs to a class of specific proteins (A β and tau being the best-characterized examples) that displays altered detergent solubility in AD, whereas other proteins (31) (including PS1) do not. Our findings are in keeping with previous work showing that glial

fibrillary acidic protein becomes increasingly detergent insoluble in AD (31). Taken together, these findings support the idea that detergent insolubility is an aspect of the disease process not restricted to selective neuronal molecules, but also includes specific astrocytic proteins.

In contrast to detergent-insoluble EAAT2, detergent-soluble EAAT2 levels were reduced in AD patients compared with normal controls. These data are in keeping with previous human studies (6–8) and in findings from 2 AD mouse models (32, 33). Protein detergent insolubility does not seem to be recapitulated in AD mouse models (data not shown). Thus, although it is currently not possible to examine detergent insolubility in mice, the effects of AD-related pathology on soluble EAAT2/GLT-1 expression in AD patients and transgenic mice are nonetheless mutually supportive.

Our findings cannot address the mechanisms by which detergent-insoluble EAAT2 accumulates in AD. A potentially important insight comes from data showing that glutamate transporters are sensitive to biological conditions that promote reactive oxygen species (16, 34), and, significantly, oxidative stress is an early and persistent feature of AD (35). Posttranslational oxidative EAAT2 modifications inhibit glutamate uptake (16) and promote formation of detergent-insoluble high-molecular weight multimers (34). This correspondence between detergent insolubility and reduced uptake suggests the possibility that increased levels of detergent-insoluble EAAT2 observed in AD brain tissue may reflect increasing EAAT2 dysfunction. This idea is consistent with data showing that A β generates oxidative radicals that impair glutamate uptake (36, 37). In addition, A β impairs glutamate uptake in synaptosomes (9–13, 49).

Until recently, EAAT2 had been widely accepted as an astrocyte-specific glutamate transporter, but it is now clear that EAAT2 is also expressed by neurons (38). Such findings, in conjunction with a report that EAAT2 is sporadically expressed in tau-positive cortical and hippocampal neurons of some AD patients (39), raised the question as to whether increased AD-related detergent-insoluble EAAT2 reflects aberrant EAAT2 expression in neurons. We did observe EAAT2 immunoreactivity associated with apparent ghost tangles (neurofibrillary remnants of dead neurons), but the absence of EAAT2 perikaryon immunoreactivity in either AD or normal control patients was much more striking. These findings suggest that EAAT2 does not markedly accumulate in somal or proximal dendritic regions of neurons in AD. It seems more likely that detergent-insoluble EAAT2 complexes accumulate in fine perisynaptic distal astrocytic processes where most of EAAT2 is normally localized (28), but which are difficult to investigate by light microscopy. Our human postmortem specimens are not suitable for the electron microscopic approaches required to address this issue in a quantitative manner.

EAATs Regulate Multiple Critical Neuroprotective Functions in the Brain and Are Disturbed in AD

A family of 5 Na⁺-dependent high-affinity glutamate transporters (referred to as EAAT1–5, also known as GLAST,

GLT-1, EAAC1, EAAT4, and EAAT5, respectively) carries out the critical task of clearing glutamate, primarily into astrocytes, thereby maintaining glutamate at basal extracellular concentrations that recently have been estimated to be in the low nanomolar range (40). The importance of rapid clearing extracellular glutamate is illustrated by the consequences of injecting potent glutamate transport blockers in mice that die quickly of apparent acute glutamate toxicity (41). The EAAT1, EAAT2, and neuron-specific EAAT3 are the primary glutamate transporters in the hippocampus and cortex; EAAT4 is expressed primarily in the cerebellum; and EAAT5 is expressed mostly in the retina (42). Of these transporters, EAAT2 is responsible for most glutamate clearance in the forebrain and accounts for approximately 80% of the glutamate transporters in the hippocampus (28, 29). The disproportionate expression of EAAT2 compared with other glutamate transporter subtypes is reflected by the dramatic phenotype of GLT-1 KO mice, which die shortly after birth because of seizures (2). The phenotypes of EAAT1/GLAST KO and EAAT3/EAAC1 KO mice are subtler. The EAAT1/GLAST KO mice develop normally but display defects in motor coordination related to cerebellar function (43). The EAAT3/EAAC1 KO mice also breed normally but develop age-related neuronal loss (44). Nonetheless, both EAAT1 and EAAT3 expressions are disturbed in AD (6, 44–46). Thus, in addition to EAAT2, multiple members of the Na⁺-dependent glutamate transporter family may contribute to AD-related pathogenic processes.

In addition to the critical role EAAT2 plays in preventing excitotoxicity (2), EAAT2 regulates stimulus-specific synaptic plasticity (5). The loss of EAAT2 has also been shown to impair activity-dependent glucose utilization (47). Impaired EAAT2 functions, even if initially latent or mild, may synergistically combine to promote increasingly pathogenic cycles of CNS dysfunction over time. In this regard, memantine, a drug hypothesized to temper excessive NMDA receptor activation, has efficacy in treating AD (48). Such findings lend additional credence to the notion that disturbed glutamatergic signaling may have a significant role in AD pathogenesis. Our present findings offer further evidence that glutamate-related dysfunction may be an important feature of AD pathology and suggest the possibility that strategies aimed at enhancing the natural neuroprotective properties of astrocytes may open new therapeutic opportunities to treat AD.

REFERENCES

- Lipton SA. Pathologically activated therapeutics for neuroprotection. *Nat Rev Neurosci* 2007;8:803–8.
- Tanaka K, Watake K, Manabe T, et al. Epilepsy and exacerbation of brain injury in mice lacking the glutamate transporter GLT-1. *Science* 1997;276:1699–702.
- Namura S, Maeno H, Takami S, et al. Inhibition of glial glutamate transporter GLT-1 augments brain edema after transient focal cerebral ischemia in mice. *Neurosci Lett* 2002;324:117–20.
- Pardo AC, Wong V, Benson LM, et al. Loss of the astrocyte glutamate transporter GLT1 modifies disease in SOD1(G93A) mice. *Exp Neurol* 2006;201:120–30.
- Tsvetkov E, Shin RM, Bolshakov VY. Glutamate uptake determines pathway specificity of long-term potentiation in the neural circuitry of fear conditioning. *Neuron* 2004;41:139–51.
- Jacob CP, Koutsilieri E, Bartl J, et al. Alterations in expression of glutamatergic transporters and receptors in sporadic Alzheimer's disease. *J Alzheimer's Dis* 2007;11:97–116.
- Masliyah E, Alford M, DeTeresa R, et al. Deficient glutamate transport is associated with neurodegeneration in Alzheimer's disease. *Ann Neurol* 1996;40:759–66.
- Abdul HM, Sama MA, Furman JL, et al. Cognitive decline in Alzheimer's disease is associated with selective changes in calcineurin/NFAT signaling. *J Neurosci* 2009;29:12957–69.
- Guo ZH, Mattson MP. Neurotrophic factors protect cortical synaptic terminals against amyloid and oxidative stress-induced impairment of glucose transport, glutamate transport and mitochondrial function. *Cereb Cortex* 2000;10:50–57.
- Guo Z, Ersoz A, Butterfield DA, et al. Beneficial effects of dietary restriction on cerebral cortical synaptic terminals: Preservation of glucose and glutamate transport and mitochondrial function after exposure to amyloid β -peptide, iron, and 3-nitropropionic acid. *J Neurochem* 2000;75:314–20.
- Keller JN, Pang Z, Geddes JW, et al. Impairment of glucose and glutamate transport and induction of mitochondrial oxidative stress and dysfunction in synaptosomes by amyloid β -peptide: Role of the lipid peroxidation product 4-hydroxynonenal. *J Neurochem* 1997;69:273–84.
- Keller JN, Gemmeyer A, Begley JG, et al. 17 β -Estradiol attenuates oxidative impairment of synaptic Na⁺/K⁺-ATPase activity, glucose transport, and glutamate transport induced by amyloid β -peptide and iron. *J Neurosci Res* 1997;50:522–30.
- Lauderback CM, Hackett JM, Huang FF, et al. The glial glutamate transporter, GLT-1, is oxidatively modified by 4-hydroxy-2-nonenal in the Alzheimer's disease brain: The role of Abeta1–42. *J Neurochem* 2001;78:413–16.
- Haugeto O, Ullensvang K, Levy LM, et al. Brain glutamate transporter proteins form homomultimers. *J Biol Chem* 1996;271:27715–22.
- Trotti D, Rizzini BL, Rossi D, et al. Neuronal and glial glutamate transporters possess an SH-based redox regulatory mechanism. *Eur J Neurosci* 1997;9:1236–43.
- Trotti D, Rossi D, Gjesdal O, et al. Peroxynitrite inhibits glutamate transporter subtypes. *J Biol Chem* 1996;271:5976–79.
- Hughes CP, Berg L, Danziger WL, et al. A new clinical scale for the staging of dementia. *Br J Psychiatry* 1982;140:566–72.
- Ball M, Braak H, Goethe J, et al. Consensus recommendations for the postmortem diagnosis of Alzheimer's disease. The National Institute on Aging, and Reagan Institute Working Group on Diagnostic Criteria for the Neuropathological Assessment of Alzheimer's Disease. *Neurobiol Aging* 1997;18:S1–S2.
- Yang W, Woltjer RL, Sokal I, et al. Quantitative proteomics identifies surfactant-resistant α -synuclein in cerebral cortex of parkinsonism-dementia complex of Guam but not Alzheimer's disease or progressive supranuclear palsy. *Am J Pathol* 2007;171:993–1002.
- Williams SM, Sullivan RK, Scott HL, et al. Glial glutamate transporter expression patterns in brains from multiple mammalian species. *Glia* 2005;49:520–41.
- Yang Y, Kinney GA, Spain WJ, et al. Presenilin-1 and intracellular calcium stores regulate neuronal glutamate uptake. *J Neurochem* 2004;88:1361–72.
- Woltjer RL, Cimino PJ, Boutte AM, et al. Proteomic determination of widespread detergent-insolubility including A- β but not tau early in the pathogenesis of Alzheimer's disease. *FASEB J* 2005;19:1923–25.
- Field A. *Discovering Statistics Using SPSS*. 2nd Ed. London, UK: Sage Publications, 2005:777.
- Winer BJ, Brown DR, Michels KM. *Statistical Principles in Experimental Design*. 3rd Ed. New York, NY: McGraw-Hill Inc, 1991:1057.
- Yernool D, Boudker O, Jin Y, et al. Structure of a glutamate transporter homologue from *Pyrococcus horikoshii*. *Nature* 2004;431:811–18.
- Cribbs DH, Chen LS, Bende SM, et al. Widespread neuronal expression of the presenilin-1 early-onset Alzheimer's disease gene in the murine brain. *Am J Pathol* 1996;148:1797–806.
- Johnston JA, Froelich S, Lannfelt L, Cowburn RF, et al. Quantification of presenilin-1 mRNA in Alzheimer's disease brains. *FEBS Lett* 1996;394:279–84.
- Furness DN, Dehnes Y, Akhtar AQ, et al. A quantitative assessment of glutamate uptake into hippocampal synaptic terminals and astrocytes:

- New insights into a neuronal role for excitatory amino acid transporter 2 (EAAT2). *Neuroscience* 2008;157:80–94
29. Lehre KP, Danbolt NC. The number of glutamate transporter subtype molecules at glutamatergic synapses: Chemical and stereological quantification in young adult rat brain. *J Neurosci* 1998;18:8751–57
 30. Feany MB, Dickson DW. Neurodegenerative disorders with extensive tau pathology: A comparative study and review. *Ann Neurol* 1996;40:139–48
 31. Woltjer RL, Sonnen JA, Sokal I, et al. Quantitation and mapping of cerebral detergent-insoluble proteins in the elderly. *Brain Pathol* 2009;19:365–74
 32. Malm TM, Iivonen H, Goldsteins G, et al. Pyrrolidine dithiocarbamate activates Akt and improves spatial learning in APP/PS1 mice without affecting β -amyloid burden. *J Neurosci* 2007;27:3712–21
 33. Masliah E, Alford M, Mallory M, et al. Abnormal glutamate transport function in mutant amyloid precursor protein transgenic mice. *Exp Neurol* 2000;163:381–87
 34. Trotti D, Danbolt NC, Volterra A. Glutamate transporters are oxidant-vulnerable: A molecular link between oxidative and excitotoxic neurodegeneration? *Trends Pharmacol Sci* 1998;19:328–34
 35. Moreira PI, Santos MS, Oliveira CR, et al. Alzheimer disease and the role of free radicals in the pathogenesis of the disease. *CNS Neurol Disord Drug Targets* 2008;7:3–10
 36. Harris ME, Carney JM, Cole PS, et al. β -amyloid peptide-derived, oxygen-dependent free radicals inhibit glutamate uptake in cultured astrocytes: Implications for Alzheimer's disease. *Neuroreport* 1995;6:1875–79
 37. Harris ME, Wang Y, Pedigo NW Jr, et al. Amyloid β peptide (25–35) inhibits Na^+ -dependent glutamate uptake in rat hippocampal astrocyte cultures. *J Neurochem* 1996;67:277–86
 38. Chen W, Mahadomrongkul V, Berger UV, et al. The glutamate transporter GLT1a is expressed in excitatory axon terminals of mature hippocampal neurons. *J Neurosci* 2004;24:1136–48
 39. Thal DR. Excitatory amino acid transporter EAAT-2 in tangle-bearing neurons in Alzheimer's disease. *Brain Pathol* 2002;12:405–11
 40. Herman MA, Jahr CE. Extracellular glutamate concentration in hippocampal slice. *J Neurosci* 2007;27:9736–41
 41. Shimamoto K, Sakai R, Takaoka K, et al. Characterization of novel L-threo- β -benzyloxyaspartate derivatives, potent blockers of the glutamate transporters. *Mol Pharmacol* 2004;65:1008–15
 42. Danbolt NC. Glutamate uptake. *Prog Neurobiol* 2001;65:1–105
 43. Watake K, Hashimoto K, Kano M, et al. Motor discoordination and increased susceptibility to cerebellar injury in GLAST mutant mice. *Eur J Neurosci* 1998;10:976–88
 44. Aoyama K, Suh SW, Hamby AM, et al. Neuronal glutathione deficiency and age-dependent neurodegeneration in the EAAC1 deficient mouse. *Nat Neurosci* 2006;9:119–26
 45. Duerson K, Woltjer RL, Mookherjee P, et al. Detergent-Insoluble EAAC1/EAAT3 aberrantly accumulates in hippocampal neurons of Alzheimer's disease patients. *Brain Pathol* 2009;19:267–78
 46. Scott HL, Pow DV, Tannenberg AE, et al. Aberrant expression of the glutamate transporter excitatory amino acid transporter 1 (EAAT1) in Alzheimer's disease. *J Neurosci* 2002;22:RC206
 47. Voutsinos-Porche B, Bonvento G, Tanaka K, et al. Glial glutamate transporters mediate a functional metabolic crosstalk between neurons and astrocytes in the mouse developing cortex. *Neuron* 2003;37:275–86
 48. Lipton SA. Paradigm shift in neuroprotection by NMDA receptor blockade: Memantine and beyond. *Nat Rev Drug Discov* 2006;5:160–70
 49. Li S, Hong S, Shepardson NE, et al. Soluble oligomers of amyloid-beta protein facilitate hippocampal long-term depression by disrupting neuronal glutamate uptake. *Neuron* 2009;62:788–801

ARTICLE

Received 17 Sep 2010 | Accepted 12 Jan 2011 | Published 8 Feb 2011

DOI: 10.1038/ncomms1190

Glia- and neuron-specific functions of TrkB signalling during retinal degeneration and regeneration

Chikako Harada^{1,2}, Xiaoli Guo¹, Kazuhiko Namekata¹, Atsuko Kimura¹, Kazuaki Nakamura¹, Kohichi Tanaka³, Luis F. Parada² & Takayuki Harada^{1,2}

Glia, the support cells of the central nervous system, have recently attracted considerable attention both as mediators of neural cell survival and as sources of neural regeneration. To further elucidate the role of glial and neural cells in neurodegeneration, we generated TrkB^{GFP} and TrkB^{c-kit} knockout mice in which TrkB, a receptor for brain-derived neurotrophic factor (BDNF), is deleted in retinal glia or inner retinal neurons, respectively. Here, we show that the extent of glutamate-induced retinal degeneration was similar in these two mutant mice. Furthermore in TrkB^{GFP} knockout mice, BDNF did not prevent photoreceptor degeneration and failed to stimulate Müller glial cell proliferation and expression of neural markers in the degenerating retina. These results demonstrate that BDNF signalling in glia has important roles in neural protection and regeneration, particularly in conversion of Müller glia to photoreceptors. In addition, our genetic models provide a system in which glia- and neuron-specific gene functions can be tested in central nervous system tissues *in vivo*.

¹ Department of Molecular Neurobiology, Tokyo Metropolitan Institute for Neuroscience, 2-6 Musashidai, Fuchu, Tokyo 183-8526, Japan. ² Department of Developmental Biology and Kent Waldrep Foundation Center for Basic Research on Nerve Growth and Regeneration, University of Texas Southwestern Medical Center, 6000 Harry Hines Boulevard, Dallas, Texas 75390-9133, USA. ³ Laboratory of Molecular Neuroscience, School of Biomedical Science and Medical Research Institute, Tokyo Medical and Dental University, Tokyo 113-8510, Japan. Correspondence and requests for materials should be addressed to L.F.P. (email: luis.parada@utsouthwestern.edu) or to T.H. (email: harada-tk@igakuken.or.jp).

In the central nervous system (CNS), glial cells have long been thought to simply provide scaffolding and physical support for neurons, whose electrical impulses underlie all sensation, movement and thought. However, recent studies have demonstrated that glia, which account for 90% of the cells in some regions of the human brain, have more significant roles than previously hypothesized¹. For example, glial cells guide migrating neurons to their destinations, control synapse number and may participate in the homeostatic activity-dependent regulation of synaptic connectivity^{2,3}. In addition, radial glial cells, which express a number of markers also expressed by neural progenitors, were demonstrated to dedifferentiate, proliferate and give rise to neurons *in vivo*^{4–6}. We previously demonstrated that the glutamate transporter GLAST, one such progenitor marker⁷, is expressed in retina-specific Müller glial cells, which are thought to carry out many of the functions of radial glia, astrocytes and oligodendrocytes in the CNS^{8,9}. Müller glial cells dedifferentiate in response to neurotoxic damage or injury, implying that even the adult mammalian retina may have regenerative potential^{10,11}. The response of Müller glia to acute retinal damage may be mediated by growth factors produced by retinal cells, such as basic fibroblast growth factor (bFGF) and brain-derived neurotrophic factor (BDNF)^{12–14}. BDNF is known to regulate neural cell survival and axonal outgrowth mainly by activating TrkB receptors, which stimulates various signalling cascades, such as mitogen-activated protein kinase pathway, phosphatidylinositol 3-kinase pathway and Fyn-mediated actin polymerization^{15–17}. However, TrkB expression is low in photoreceptors relative to other retinal cell types, including retinal ganglion cells (RGCs) and Müller glia^{12,13,18}. Consequently, we previously proposed a model in which exogenously applied or microglia-derived neurotrophins regulate photoreceptor survival indirectly by regulating secondary trophic factor production in Müller glia^{12,19}. However, the effects that such a glia-neuron interaction would have *in vivo* or whether it would be relevant for the protection of neural cell types that express TrkB remained unclear.

In the present study, we prepared two conditional knockout (KO) mice in which TrkB was deleted from retinal glia or from two types of retinal neurons (RGCs and amacrine cells). These mice enabled us to separately examine direct and indirect effects of TrkB on neuroprotection. We demonstrate that TrkB signalling in Müller glia is critically involved in neural protection and regeneration during retinal degeneration. These mice may enable the further study of genes involved in the glia-neuron network and neurodegeneration.

Results

Glia- and neuron-specific TrkB ablation in the retina. Previous studies have shown that the *GFAP-Cre* transgenic strain, in which Cre expression is regulated by the human GFAP promoter, expresses Cre recombinase not only in mature astrocytes but also in multipotent radial glial cells that exhibit neural stem/progenitor cell properties^{20,21}. To examine expression of the *GFAP-Cre* transgene in the adult retina, we crossed *GFAP-Cre* mice with a *Rosa26-LacZ* reporter line^{22,23} in which recombination results in expression of β -galactosidase (β -gal; Fig. 1a,b). To identify the specific β -gal immunopositive (IP) cell type(s), we carried out co-staining with markers of other retinal lineages. β -gal-IP cells were double labelled with glutamine synthetase (GS; a marker of Müller glial cells), but not with calretinin (a marker of RGCs and amacrine cells), calbindin (a marker of horizontal cells) or protein kinase C (PKC; a marker of bipolar cells; Fig. 1b). These results revealed that β -gal expression, which reflects Cre recombinase expression, is restricted to glial cells in *GFAP-Cre LacZ* mice. On the other hand, in *c-kit-Cre LacZ* mice²⁴, β -gal-IP cells were double labelled with calretinin and TUJ1 (another RGC marker), but not with GS, calbindin or PKC (Fig. 1b). These results indicate that, in contrast to *GFAP-Cre LacZ* mice, expression of Cre recombinase is restricted to RGCs and amacrine cells in *c-kit-Cre LacZ* mice (Fig. 1a).

To selectively eliminate TrkB from retinal glia or neurons, we next crossed *TrkB^{lox/lox}* mice²⁵ with *GFAP-Cre* or *c-kit-Cre* mice. The resulting double transgenic *TrkB^{lox/lox};GFAP-Cre+* and *TrkB^{lox/lox};c-kit-Cre+* mice were termed as *TrkB^{GFAP} KO* mice and *TrkB^{c-kit} KO* mice, respectively. Retinal development and structure were normal in both strains compared with wild-type (WT) mice (Supplementary Fig. S1). Immunohistochemical analysis revealed that TrkB protein expression in Müller glia (arrowheads in Fig. 1c) was eliminated in *TrkB^{GFAP} KO* mice. In contrast, TrkB expression was eliminated in RGCs (arrowheads in Fig. 1d) and amacrine cells (arrows in Fig. 1d) in *TrkB^{c-kit} KO* mice. Taken together, these findings demonstrate that *GFAP-Cre* and *c-kit-Cre* virtually eliminated TrkB expression from retinal glia and neurons, respectively.

Direct and indirect effects of BDNF on RGC protection. Neurotrophins prevent RGC death from glutamate neurotoxicity²⁶. As RGCs express TrkB receptors, we compared the roles of TrkB signalling in RGCs and Müller glia in BDNF-dependent neuroprotection to determine the direct and indirect effects, respectively. For this purpose, we prepared retinal explants from WT, *TrkB^{c-kit} KO* and *TrkB^{GFAP} KO* mice (Fig. 2a). The WT retinal explants stimulated with 5 mM glutamate for 1 h showed a decrease in the number of NeuN-positive neurons in the ganglion cell layer (GCL) compared with the untreated control explants (Fig. 2a,b). As expected, the same treatment significantly decreased the number of surviving RGCs in the *TrkB^{c-kit} KO* mouse retina. We predicted milder RGC degeneration in the *TrkB^{GFAP} KO* compared with the *TrkB^{c-kit} KO* mouse retina; however, RGC loss was as severe as that observed in the *TrkB^{c-kit} KO* mouse retina (Fig. 2a,b). These results suggest that, at least under our experimental conditions, the indirect protective effect of BDNF by Müller glia is as powerful as the direct effect through TrkB in RGCs.

To further examine the function of TrkB signalling in retinal glia, we next prepared cultured Müller cells from WT and *TrkB^{GFAP} KO* mice and analysed them by western blot. Consistent with the immunohistochemical results (Fig. 1c), TrkB protein expression in Müller glia was not detectable in *TrkB^{GFAP} KO* mice (Fig. 3a). We next examined whether exogenous BDNF stimulates TrkB-dependent signal transduction in Müller glia by observing the activation of cyclic AMP response element-binding (CREB) protein. In WT Müller cells, the basal phosphorylated CREB (pCREB) expression level was very low, but BDNF clearly increased the ratio of pCREB to CREB (Fig. 3b). In contrast, the effect of BDNF on CREB activation was only marginal in *TrkB^{GFAP} KO* Müller cells (Fig. 3b). We also examined the effect of BDNF on CREB phosphorylation *in vivo*. In WT retinas, intraocular injection of BDNF induced pCREB expression in RGCs and Müller glia (arrow and arrowhead in Fig. 3c). In *TrkB^{GFAP} KO* mice, BDNF-induced pCREB expression in RGCs was comparable with WT retinas, but expression was barely detectable in Müller glia (Fig. 3c). These results confirmed a lack of TrkB-dependent signal transduction in Müller glia in *TrkB^{GFAP} KO* mice. We previously demonstrated that treatment of cultured rat Müller cells with BDNF increases the production of several trophic factors that can protect retinal neurons¹⁹. Similarly, in mouse Müller cells, BDNF increased mRNA expression levels of BDNF, bFGF, ciliary neurotrophic factor and glial cell line-derived neurotrophic factor (Fig. 3d). However, BDNF failed to stimulate the production of trophic factors in Müller cells prepared from *TrkB^{GFAP} KO* mice (Fig. 3d). Thus, TrkB elimination in Müller glia impairs the transcription of trophic factors, which may lead to RGC vulnerability during glutamate neurotoxicity.

Accelerated photoreceptor degeneration in *TrkB^{GFAP} KO*. Various trophic factors rescue photoreceptors during retinal degeneration^{27–29}. As photoreceptors do not express a high level of neurotrophin receptors, the indirect glia-mediated rescue pathway may be more important for photoreceptors than for other cell types,

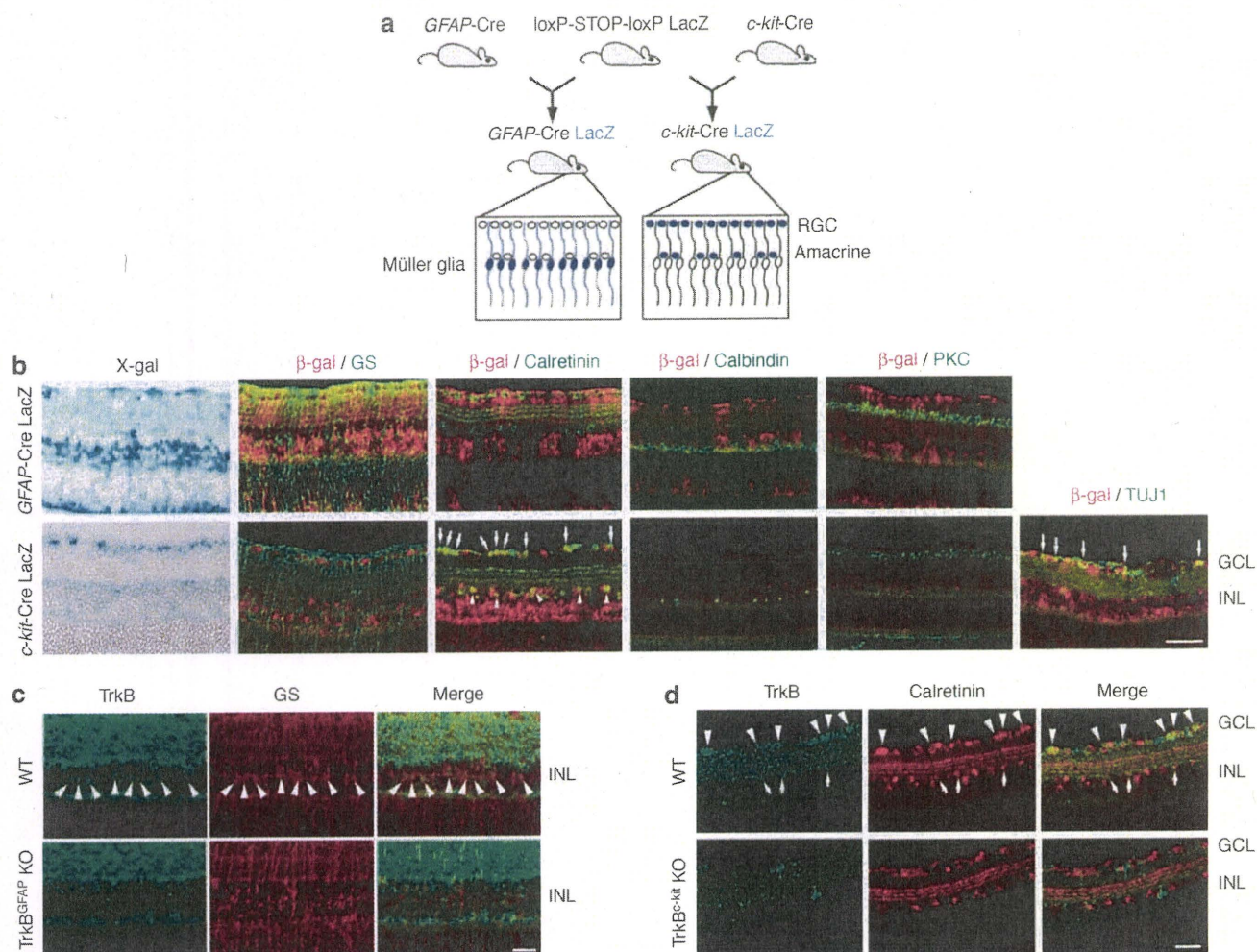


Figure 1 | Establishment of glia- and neuron-specific TrkB conditional KO mice. (a) Schematic diagram of transgenically targeted fate-mapping strategy. *GFAP-Cre* and *c-kit-Cre* mice were crossed with *Rosa26-LacZ* reporter mice. In Cre reporter offspring, only cells that express Cre excise a loxP-flanked stop signal and activate constitutive LacZ expression. Blue colour depicts LacZ-positive cells. (b) X-gal staining (blue) and immunostaining (red) of β -gal-positive cells. Glutamine synthetase (GS), calretinin, calbindin, protein kinase C (PKC) and TUJ1 were used as cell type-specific markers (green). Overlapping immunoreactivities (yellow) of β -gal and GS, calretinin or TUJ1 indicate that Cre-mediated recombination occurs in Müller glial cells in *GFAP-Cre LacZ* mice, and RGCs (arrows) and amacrine cells (arrowheads) in *c-kit-Cre LacZ* mice. (c) Immunohistochemical analysis of TrkB (green) and GS (red) showed loss of TrkB from Müller glial cells (arrowheads) in *TrkB^{GFAP} KO* mice. (d) Immunohistochemical analysis of TrkB (green) and calretinin (red) showed loss of TrkB from RGCs (arrowheads) and amacrine cells (arrows) in *TrkB^{c-kit} KO* mice. Scale bar, 100 μ m. GCL, ganglion cell layer; INL, inner nuclear layer; RGC, retinal ganglion cell.

including RGCs^{12,13,18}. To further elucidate the effect of the glia-neuron network in neuroprotection *in vivo*, we used a second animal disease model, *N*-methyl-*N*-nitrosourea (MNU)-induced photoreceptor degeneration (Fig. 4a). MNU is an alkylating agent that causes DNA methylation and activates caspases, leading to photoreceptor apoptosis in various animal species³⁰. In WT mice, 15 mg kg⁻¹ MNU decreased the thickness of the outer nuclear layer (ONL), but intravitreal injection of BDNF partially rescued the photoreceptor loss (Fig. 4b,c). However, in *TrkB^{GFAP} KO* mice, 7.5 mg kg⁻¹ MNU resulted in an ~50% loss of the ONL, which was significantly greater than the loss in WT retinas, and BDNF failed to induce photoreceptor survival against any doses of MNU (Fig. 4b,c). The protective effect of BDNF in WT mice diminished in the presence of a higher dose of MNU (60 mg kg⁻¹); this dose completely abolished the ONL but left the inner retinal layer (IRL) intact (Fig. 4b,d). In contrast, the same dose of MNU applied to *TrkB^{GFAP} KO* mice induced considerable loss of the IRL as well as the removal of the ONL (Fig. 4b,d). These *in vivo* data suggest that glial TrkB signalling has a pivotal role in the protection of surrounding neurons.

Regenerative capacity of Müller glia through TrkB signalling. Recent studies have provided evidence that radial glia sustain neural regeneration even in the adult brain⁴⁻⁶. Müller glia are considered to be a type of radial glia that may function as retinal progenitor cells^{10,11}. We therefore examined the regenerative response of Müller cells to BDNF in the MNU-induced photoreceptor degeneration model (Fig. 5a). To observe dividing cells, we labelled WT and *TrkB^{GFAP} KO* animals with 5-bromodeoxyuridine (BrdU). Although few BrdU-labelled cells were detected at day 5, intraocular injection of BDNF clearly increased BrdU-labelling in GLAST-IP cells in the inner retina (arrows) and in some cells in the ONL (Fig. 5b). In contrast, BDNF injection did not promote BrdU incorporation in *TrkB^{GFAP} KO* mice or WT mice treated with K252a, an inhibitor of Trk receptors (Fig. 5b). At day 7, BDNF-induced BrdU-positive cells were detected predominantly in the remaining ONL, where they were co-labelled with rod photoreceptor markers, such as rhodopsin and recoverin (Fig. 5c). However, BDNF-induced BrdU incorporation was suppressed in *TrkB^{GFAP} KO* mice (Supplementary Fig. S2). Furthermore, these BrdU-labelled cells were overlapped with β -gal

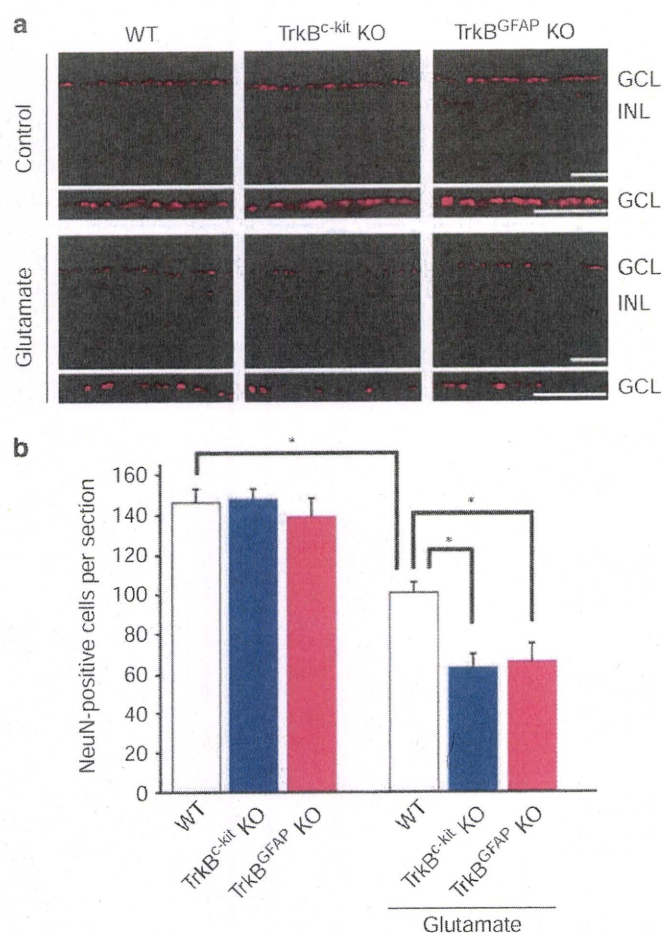


Figure 2 | Similar susceptibility to glutamate neurotoxicity in TrkB^{c-kit} KO and TrkB^{GFAP} KO retinas. (a) Immunohistochemical analysis of mouse retinal explants from WT, TrkB^{c-kit} KO and TrkB^{GFAP} KO mice stained with an anti-NeuN antibody. Explants were untreated (control) or treated with 5 mM glutamate for 1 h. Scale bar, 50 μm. (b) Quantification of NeuN-positive cells in the GCL. Data are shown as the mean ± s.e.m. (n = 6). *P < 0.01. GCL, ganglion cell layer; INL, inner nuclear layer.

staining in GFAP-Cre LacZ mice, providing evidence that they were derived from Müller glia (Fig. 5c). In addition, some BrdU-positive cells were detected in the inner retina and double labelled with Brn3b (another RGC marker) or calretinin (Fig. 5d). These results suggest the possibility that BDNF can convert the proliferating Müller glia to rod photoreceptors and, to a lesser extent, to other retinal neurons in the MNU model. Thus, TrkB deficiency achieved by Cre-mediated recombination results in the loss of regenerating Müller cells.

We further examined the effects of BDNF on cultured Müller cells and found increased nestin expression, a neural stem/progenitor cell marker, in WT but not in TrkB^{GFAP} KO Müller cells (Fig. 6a). When neural stem cells are induced to differentiate into the neurogenic pathway, *Mash1*, a proneural gene, is derepressed through a signalling cascade that depends on expression of the calcium/calmodulin-dependent protein kinase IIδ (CaMKIIδ)^{31,32}. In the retina, *Mash1* is involved in the generation of bipolar cells and photoreceptors from progenitor cells^{33,34}. A previous study showed that CaMKIIδ mediates the phosphorylation of Hes1, which is required for *Mash1* activation³¹. As BDNF can stimulate CaMKII through TrkB¹⁶, we next examined whether BDNF regulates this pathway in neural regeneration. We found that BDNF increased *Mash1* levels in WT but not in TrkB^{GFAP} KO Müller cells, and the subsequent quantitative analysis revealed that BDNF had no effect on Hes1 expression

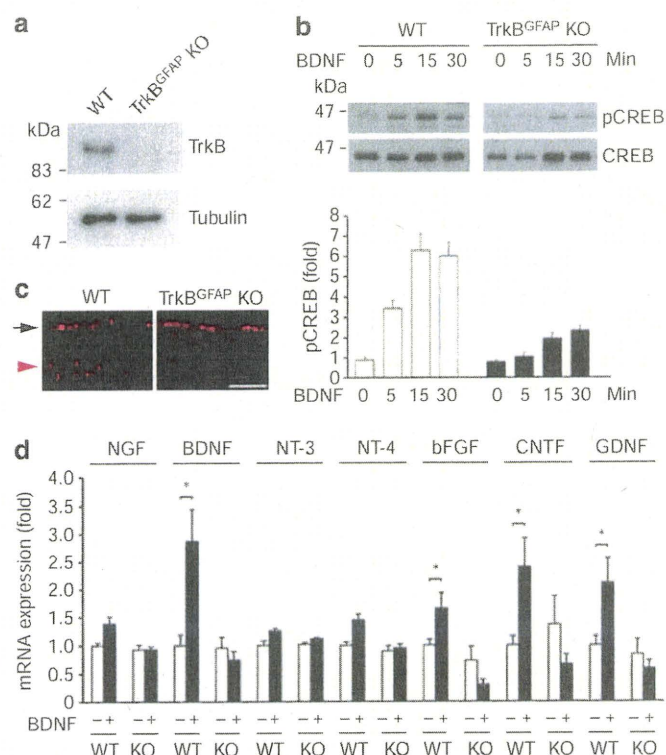


Figure 3 | Functional analysis of Müller glial cells in TrkB^{GFAP} KO mice.

(a) Immunoblot analysis of TrkB protein in cultured Müller cells from WT and TrkB^{GFAP} KO mice. (b) Immunoblot analysis of phosphorylated CREB (pCREB) and total CREB in cultured Müller cells from WT and TrkB^{GFAP} KO mice. BDNF (50 ng ml⁻¹)-induced CREB phosphorylation was impaired in TrkB^{GFAP} KO Müller cells. For each determination, the ratio of pCREB/CREB protein level in controls (WT, BDNF 0 min) was normalized to a value of 1.0. Data are shown as the mean ± s.e.m. (n = 3). (c) Immunohistochemical analysis of pCREB in BDNF (1 μg μl⁻¹)-treated WT and TrkB^{GFAP} KO retinas. Note the absence of pCREB in Müller cells (red arrowhead) of the TrkB^{GFAP} KO retina, despite its persistence in the GCL (arrow). Scale bar, 50 μm. (d) Effect of BDNF (100 ng ml⁻¹ for 48 h) on trophic factor production in cultured Müller cells from WT and TrkB^{GFAP} KO mice. For each determination, the mRNA level in controls (WT, without BDNF) was normalized to a value of 1.0. Data are shown as the mean ± s.e.m. (n = 6). *P < 0.05. NGF, nerve growth factor; NT-3, neurotrophin-3; NT-4, neurotrophin-4; CNTF, ciliary neurotrophic factor; GDNF, glial cell line-derived neurotrophic factor.

(Fig. 6b,c). In addition, BDNF significantly increased the expression level of CaMKIIδ but not CaMKIIα, CaMKIIβ or CaMKIIγ in WT Müller cells (Fig. 6d). The BDNF-induced increase of CaMKIIδ was not detected in TrkB^{GFAP} KO Müller cells (Fig. 6d). In contrast, platelet-derived growth factor, which can also activate CaMKII (ref. 31), increased nestin and *Mash1* expression in both WT and TrkB^{GFAP} KO Müller cells (Fig. 6e,f). These results suggest that BDNF signalling through TrkB stimulates the CaMKIIδ-*Mash1* pathway, which induces the potential capacity of Müller glia as intrinsic retinal progenitor cells.

Discussion

In the present study, we used TrkB^{GFAP} and TrkB^{c-kit} KO mice to explore TrkB functions in retinal Müller glia and inner retinal neurons, respectively. We observed that the extent of glutamate-induced retinal degeneration was almost equal in these two mutant mouse models. In addition, BDNF failed to prevent photoreceptor degeneration in TrkB^{GFAP} KO mice. These findings represent the first direct evidence for a role of neurotrophin receptors in glial cells during retinal degeneration. Our results are consistent with the previous

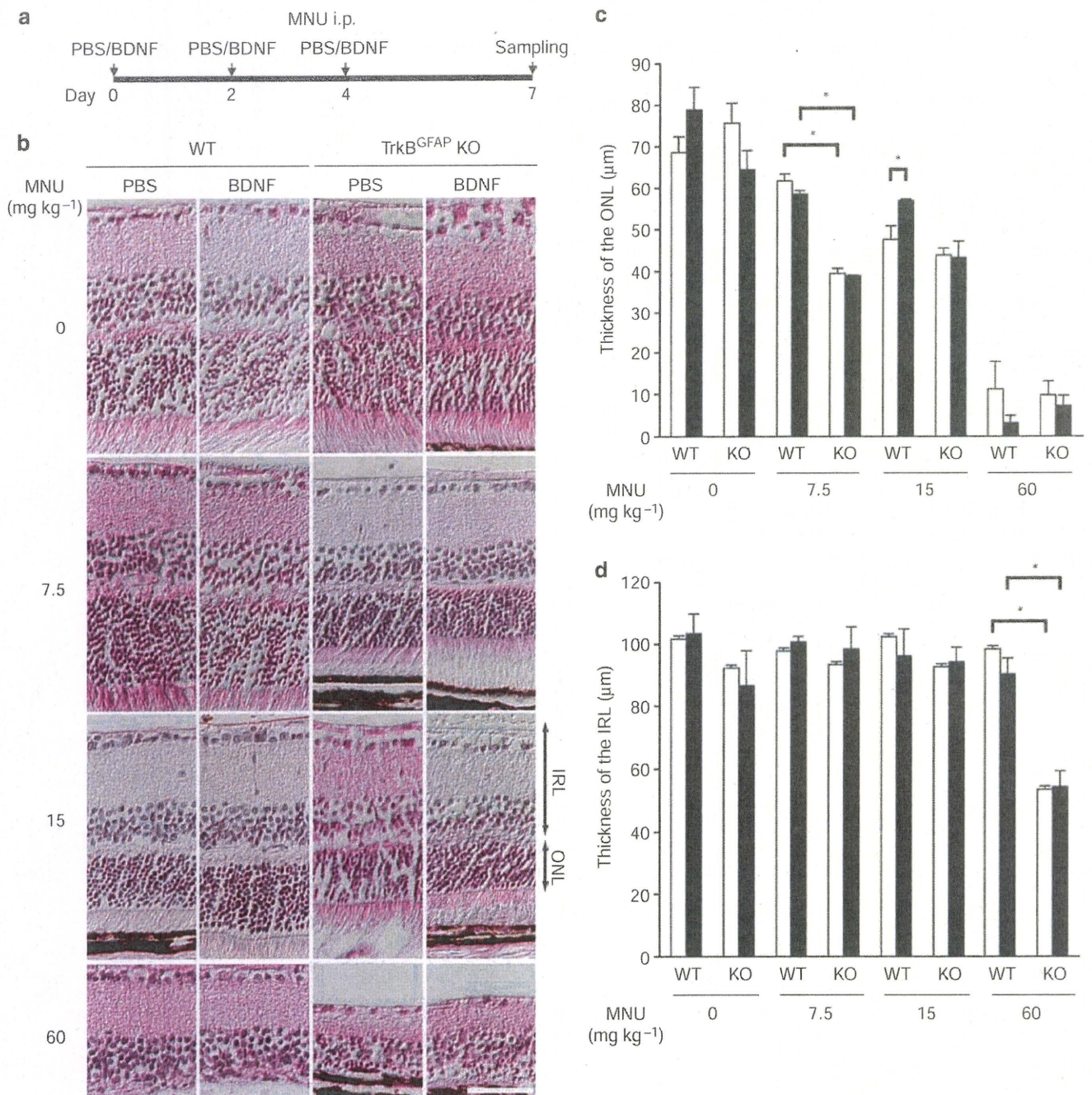


Figure 4 | Accelerated photoreceptor degeneration in TrkB^{GFAP} KO mice. (a) Animal protocols for MNU-induced photoreceptor degeneration. MNU was injected intraperitoneally (i.p.) into WT and TrkB^{GFAP} KO mice at the concentration of 0, 7.5, 15 or 60 mg kg⁻¹. PBS or BDNF (1 μg μl⁻¹) was intraocularly injected at day 0, 2 and 4, and the animals were killed at day 7 after MNU treatment. (b) Representative photomicrographs of PBS- or BDNF-treated retinas from WT and TrkB^{GFAP} KO mice administered with various concentrations of MNU. Scale bar, 50 μm. (c, d) Quantitative analysis of the thickness of the ONL (c) and the IRL (d) in PBS (white bar)- or BDNF (black bar)-treated retinas. Data are shown as the mean + s.e.m. (n = 4). *P < 0.05. IRL, inner retinal layer; ONL, outer nuclear layer.

assumption that the glia-neuron network is heavily involved in the protection of surrounding neurons *in vivo*^{12–14,19}. Another intriguing result is that BDNF–TrkB signalling stimulated Müller cells to proliferate and express retinal neural cell markers. This finding supports previous work, suggesting that Müller cells have regenerative potential^{10,11}. Thus, both BDNF stimulation and intrinsic signal transduction through TrkB may be required for Müller glia to become endogenous retinal progenitor cells. As BDNF induces the production of various trophic factors in Müller cells, including bFGF and insulin growth factor, the regeneration process may involve these trophic factors by an autocrine process. Taken together, our results

suggest that neurotrophin signalling in glia is an important mediator of neuroprotection as well as a signalling cue to induce regeneration of radial glia *in vivo*.

In the retina, glutamate excitotoxicity and oxidative stress may contribute to various eye diseases, including retinal ischaemia and glaucoma^{8,9,35–38}. In these disorders, loss of RGCs and subsequent optic nerve degeneration are the primary concerns. As RGCs express Trk receptors, neurotrophins are thought to directly regulate RGC number during development and prevent RGC death in the adult retina³⁴. However, our results suggest an unexpectedly powerful neuroprotective effect of TrkB signalling in Müller glia.

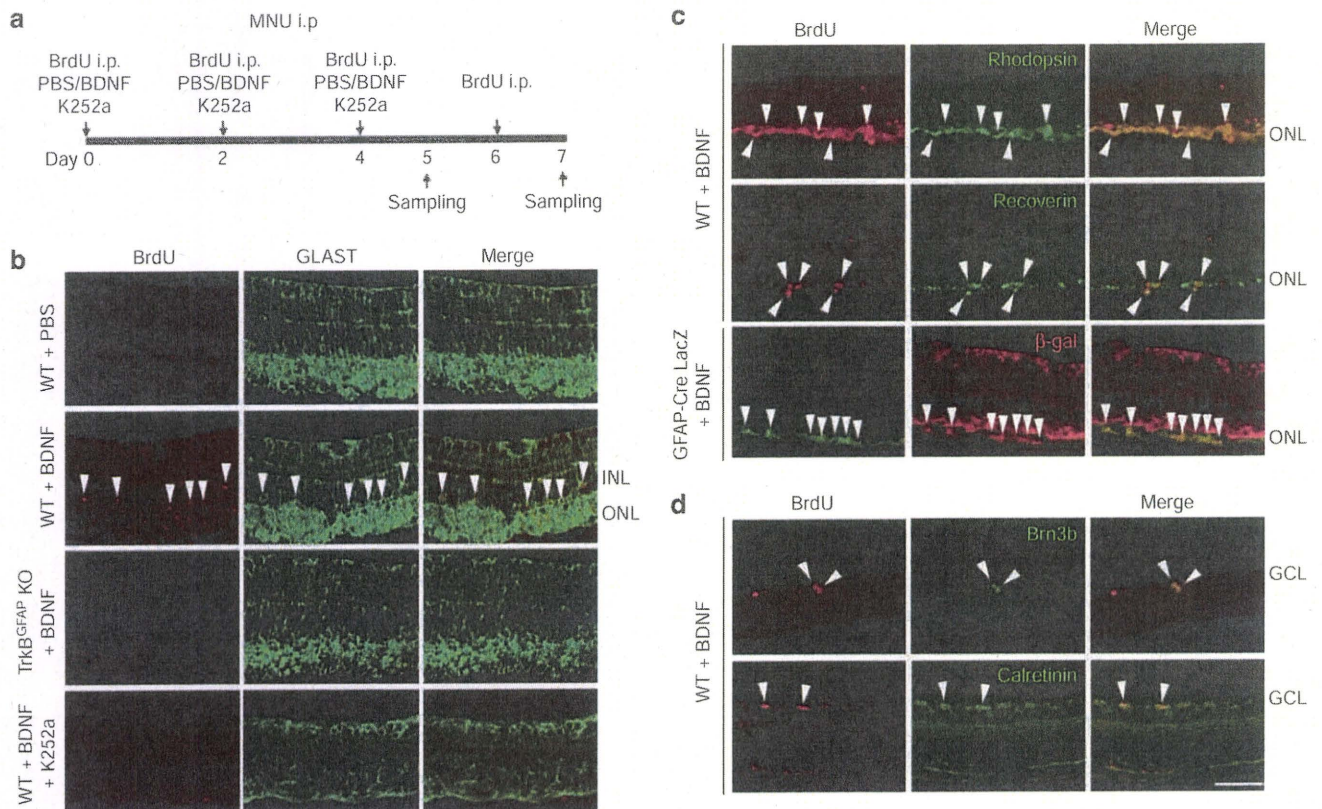


Figure 5 | Effect of BDNF on the proliferation of Müller glial cells during retinal degeneration. (a) Animal protocols. MNU (60 mg kg^{-1}) was injected intraperitoneally (i.p.) to WT, $\text{TrkB}^{\text{GFAP}}$ KO and GFAP-Cre LacZ mice. BrdU (50 mg kg^{-1}) was injected (i.p.) at day 0, 2, 4 and 6 after MNU treatment. PBS, BDNF ($1 \mu\text{g } \mu\text{l}^{-1}$) and K252a (1 mM) were intraocularly injected at day 0, 2 and 4, and the animals were killed at day 5 or 7. (b) Sections of the retina treated with PBS, BDNF and K252a in WT and $\text{TrkB}^{\text{GFAP}}$ KO mice (day 5). BDNF increased BrdU-labelling in GLAST-positive cells in the INL (arrowheads) and some cells in the ONL in WT, but not in $\text{TrkB}^{\text{GFAP}}$ KO mice. K252a (a blocker for Trk receptors) inhibited BDNF-induced BrdU expression. (c) BrdU-labelled cells in the ONL were double labelled (arrowheads) with rhodopsin or recoverin in WT mice, and with β -gal in GFAP-Cre LacZ mice (day 7). (d) BrdU-labelled cells in the GCL were double labelled (arrowheads) with Brn3b or calretinin (day 7). Scale bar, $50 \mu\text{m}$. GCL, ganglion cell layer; INL, inner nuclear layer; ONL, outer nuclear layer.

One possible explanation for this phenomenon is that the total neuroprotective effect of Müller glia-derived trophic factors (Fig. 3d) is as effective as that of direct BDNF signalling in RGCs (Fig. 2) (ref. 39). Consistently, transcorneal electrical stimulation, which stimulates Müller cell production of insulin growth factor-1 and BDNF, rescues axotomized RGCs and improves retinal function in human patients^{40,41}. Although the number is small compared with Müller glia, we cannot exclude the possibility that astrocytes located in the GCL may also be involved in RGC rescue.

Compared with RGC degeneration, photoreceptor degeneration is a relatively simple disease model in which to explore TrkB function, because TrkB expression is low in photoreceptors^{12,13,18}. In the present study, using the $\text{TrkB}^{\text{GFAP}}$ KO mouse, we demonstrated a functional glia-neuron network during photoreceptor degeneration *in vivo*. As BDNF increases ciliary neurotrophic factor and glial cell line-derived neurotrophic factor production in WT, but not in TrkB-deficient Müller cells (Fig. 3d), which can directly protect photoreceptors as well as RGCs^{12,19,27}, BDNF seems to exert photoreceptor protection by a paracrine mechanism. Consistently, MNU-induced photoreceptor degeneration was observed at a lower dose in $\text{TrkB}^{\text{GFAP}}$ KO mice compared with WT mice, and BDNF failed to prevent or delay the degeneration process in the mutant (Fig. 4). Moreover, we found that MNU induced unusual thinning of IRLs in $\text{TrkB}^{\text{GFAP}}$ KO animals (Fig. 4). These results again suggest the importance of glial TrkB signalling for the protection of various types of surrounding neurons during retinal degeneration. One may find that the protective effects of exogenous BDNF observed in our study are small.

As our MNU model is a relatively acute model, it is possible that exogenous BDNF may be more effective in other models that represent milder, slow-progressive photoreceptor degeneration.

We also examined the effect of BDNF on Müller glial cells as intrinsic retinal progenitor cells. We found that BDNF-TrkB signalling stimulated the CaMKII δ -Mash1 pathway and induced the expression of rod photoreceptor markers in proliferating Müller cells (Figs 5 and 6). This finding is consistent with the previous work that Mash1 is involved in the generation of photoreceptors from retinal progenitor cells^{33,34}. A recent study demonstrated that exogenous Wnt3a increases the proliferation of Müller cells in the photoreceptor-damaged adult mouse retina⁴². As Wnt modulates CaMK activity⁴³, Wnt signalling may promote adult neurogenesis, at least partly, through the CaMKII δ -Mash1 pathway. In fact, CaMKII activation restored the regeneration capability in the TrkB-deficient Müller cells (Fig. 6e,f). CaMK is a calcium-dependent kinase and activation of CaMK can in turn lead to phosphorylation of CREB⁴⁴. In our $\text{TrkB}^{\text{GFAP}}$ KO mice, BDNF-induced CREB phosphorylation was almost absent in Müller cells, whereas it was clearly detectable in RGCs (Fig. 3c). In astrocytes, TrkB-T1, a truncated form of TrkB that lacks tyrosine kinase activity, may mediate calcium signalling⁴⁵. However, both full-length and truncated forms of TrkB are deleted in our $\text{TrkB}^{\text{GFAP}}$ KO mice²⁵, and thus, we have not been able to determine which form of TrkB is necessary for the proliferation and differentiation of Müller cells. Further investigation into subtype-specific TrkB functions in Müller cells may lead to the identification of relevant secondary trophic factors and mechanisms

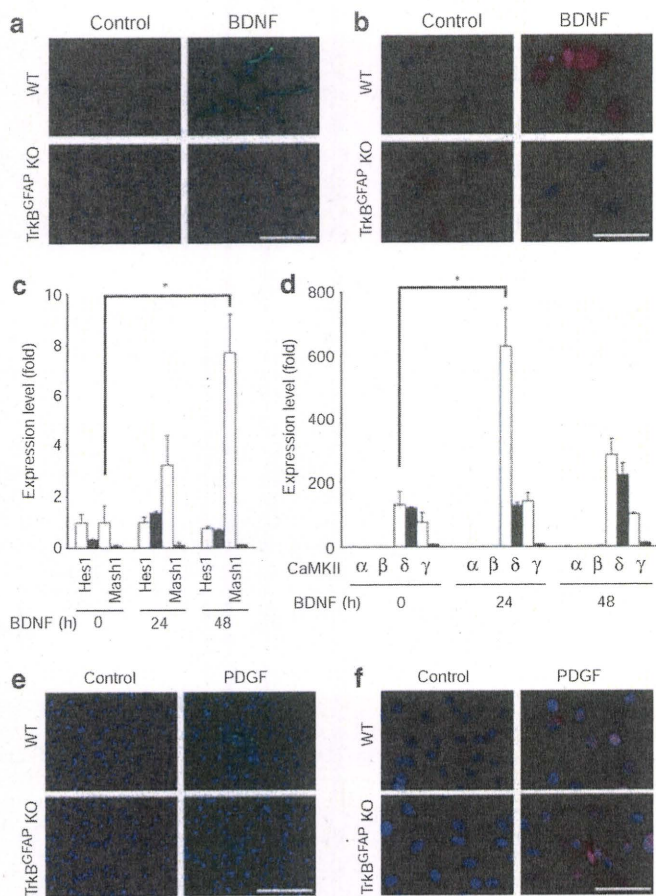


Figure 6 | Regenerative capacity of Müller glial cells mediated by TrkB signalling. (a, b) Treatment with BDNF (100 ng ml⁻¹ for 1–2 days) induced expression of nestin (a) and Mash1 (b) in cultured Müller cells from WT but not TrkB^{GFAP} KO mice. (c, d) Expression of Hes1 and Mash1 (c) and CaMKII (d) in BDNF-treated Müller cells from WT (white bar) and TrkB^{GFAP} KO (black bar) mice. Note the upregulation of CaMKIIδ and Mash1 in WT but not TrkB^{GFAP} KO Müller cells. Data are shown as the mean ± s.e.m. (n = 4). *P < 0.01. (e, f) Treatment with platelet-derived growth factor (PDGF; 50 ng ml⁻¹ for 24 h) induced expression of nestin (e) and Mash1 (f) in cultured Müller cells from WT and TrkB^{GFAP} KO mice. Scale bars, 150 μm (a, e) and 50 μm (b, f).

of effective regeneration in the degenerating retina. We also showed that BDNF induces the expression of RGC markers in proliferating, that is, BrdU-positive, cells in MNU-treated mice (Fig. 5). However, the rate of occurrence and the number of identified cells were much lower than those for photoreceptor markers. It is possible that degenerating photoreceptors in MNU-treated mice may release trophic factors⁴⁶, including bFGF, which could act in combination with BDNF to stimulate Müller cell proliferation in the ONL. However, this study clearly demonstrates that BDNF–TrkB signalling is one of the active pathways involved in Müller glial cell regeneration. Additional RGC degeneration models and further TrkB signalling and effector pathway studies may lead to better understanding of the mechanisms and transcriptional regulators at play.

In summary, we report important roles of neurotrophin signalling in glial cells as well as in neural cells. Loss of TrkB signalling in glial cells led to severe retinal degeneration in two different animal models. In addition, BDNF–TrkB signalling stimulated the proliferation and differentiation of dedifferentiated Müller glial cells in the degenerating retina. Our glia- and neuron-specific KO mice offer a powerful system for investigating region-specific functions of target genes as well as their contributions to the glia-neuron network

in vivo. Recent studies have shown that the unprocessed precursor forms of neurotrophin family members, for example, proBDNF, are released from neurons during development and in adulthood, and such molecules can act through a co-receptor system of p75^{NTR} and sortilin^{47,48}. Thus, further study is required to determine whether Müller glia-derived BDNF includes proBDNF and, if so, whether proBDNF induces neural cell apoptosis or inhibits the regenerative potential of Müller cells *in vivo*.

Methods

Mice. Experiments were performed using TrkB^{lox/lox};GFAP-Cre+ (TrkB^{GFAP} KO) and TrkB^{lox/lox};c-kit-Cre+ (TrkB^{c-kit} KO) mice^{23,24,25} in accordance with the Tokyo Metropolitan Institute for Neuroscience Guidelines for the Care and Use of Animals. Light intensity inside the cages ranged from 100 to 200 lux under a 12 h light/12 h dark cycle.

Histological and morphometric studies. Paraffin sections (7 μm thick) were cut through the optic nerve and stained with hematoxylin and eosin. The sections were examined with a Microscope (BX51; Olympus) equipped with Plan Fluor objectives connected to a DP70 camera (Olympus). The number of cells in the GCL was counted from one ora serrata through the optic nerve to the other ora serrata³⁷. The thickness of the ONL and IRL (between the internal limiting membrane and the interface of the outer plexiform layer and INL) was measured using NIH Image (ImageJ 1.38) (ref. 12). Immunohistochemistry was performed using a Rabbit antibody against TrkB (1:200, Santa Cruz) and a Mouse antibody against GS (1:500, Chemicon) or Calretinin (1:500, Chemicon).

β-gal expression in GFAP-Cre LacZ and c-kit-Cre LacZ mice. Frozen retinal sections were incubated in X-gal solution at 37 °C for 12 h (ref. 23). For double-labelling immunohistochemistry, the sections were incubated with a Goat polyclonal antibody against β-gal (1:1,000, Biogenesis) and a Mouse antibody against GS (1:500, Chemicon), Calretinin (1:500, Chemicon), PKC (1:500, Sigma), Calbindin (1:100, Sigma) or TUJ1 (1:100, R&D).

Retinal explant culture. The neural retina without pigment epithelium was placed on a Millicell chamber filter (30-mm diameter, pore size 0.4 μm; Millipore) with the GCL upwards. The chambers were transferred to a 6-well culture plate, with each well containing 1 ml of DMEM/F-12 (Invitrogen) containing 20% Heat-inactivated horse serum (Invitrogen), changed every other day. The cells were cultured at 34 °C in 5% CO₂. Retinal explant cultures were incubated with or without 5 mM glutamate for 1 h. After 72 h, retinal explants were immunostained with Mouse anti-NeuN (1:1,000, Chemicon), and the number of NeuN-positive cells in the GCL was quantified⁴⁹.

Müller cell proliferation during photoreceptor degeneration. MNU was injected intraperitoneally (i.p.) into WT, TrkB^{GFAP} KO and GFAP-Cre LacZ mice at the concentration of 7.5, 15 or 60 mg kg⁻¹. BrdU was injected (i.p.) at a dose of 50 mg kg⁻¹ at day 0, 2, 4 and 6 after MNU treatment. BDNF (1 μg μl⁻¹) and K252a (1 mM, Alomone Labs) were intraocularly injected at day 0, 2 and 4. At day 5 or 7, the animals were killed, and retinal sections were stained with Mouse anti-BrdU (1:20, Roche) and Rabbit anti-GLAST (1:1,000)⁸, Rabbit anti-Recoverin (1:1,000, Millipore), Goat anti-β-gal (1:1,000, Biogenesis) or Goat anti-Brn3b (1:200, Santa Cruz) antibodies. Some sections were stained with Rat anti-BrdU (1:40, Abcam) and Mouse anti-Rhodopsin (1:1,000, Sigma) or Mouse anti-Calretinin (1:500, Chemicon) antibodies. The number of BrdU-positive or BrdU/rhodopsin-double positive cells was counted from one ora serrata through the optic nerve to the other ora serrata³⁷.

Müller cell culture. Primary Müller cells¹⁹ were treated with 50 ng ml⁻¹ of BDNF for 0–0.5, 12 or 24 h, and 50 ng ml⁻¹ of platelet-derived growth factor for 24 h. Immunocytochemical analysis was performed with Mouse anti-Nestin (1:100, Chemicon) and Rabbit anti-Mash1 (1:40, R&D) antibodies, followed by 4,6-diamidino-2-phenylindole staining. Total RNA was extracted with Isogen (Nippon Gene) according to the manufacturer's protocol. Resultant RNA was treated with DNase (RQ1 RNase-Free DNase; Promega) and reverse-transcribed with Revertra ace (Toyobo) to obtain cDNA. Quantitative reverse transcription PCR was performed using the ABI 7500 fast real-time PCR system with SYBR Green PCR Master Mix (Applied Biosystems)⁵⁰. Thermo cycling of each reaction was performed with each primer at a concentration of 100 nM. The following protocol was used: denaturation programme (95 °C for 3 min), followed by the amplification and quantification programme (95 °C for 15 s and 60 °C for 30 s) repeated for 50 cycles. The PCR quality and specificity were verified by melting curve analysis. A standard curve of cycle thresholds using serial dilutions of cDNA samples were used to calculate the relative abundance. The difference in the initial amount of total RNA between the samples was normalized in every assay using glyceraldehyde-3-phosphate dehydrogenase (GAPDH) gene expression as an internal standard. The primer probe pairs used are listed in Supplementary Table S1.

Immunoblotting. Cultured Müller cells were homogenized in ice-cold 50 mM Tris-HCl (pH 7.4) containing 150 mM NaCl, 0.1% Triton X-100 and a protease inhibitor cocktail (Roche). Protein concentrations were determined using a Bio-Rad protein assay kit (Bio-Rad). Samples were separated on SDS polyacrylamide gel electrophoresis gels and subsequently electrotransferred to Immobilon-P filter (Millipore). Membranes were incubated with Rabbit antibodies against TrkB (1:200, Santa Cruz), Tubulin (1:1,000, Cell Signaling), CREB (1:1,000, Cell Signaling) or pCREB (1:1,000, Cell Signaling). Primary antibody binding was detected using horseradish peroxidase-labelled anti-Mouse IgG secondary antibody (Amersham) and visualized using ECL Plus western blotting system (Amersham).

Statistical analyses. Data are presented as means \pm s.e.m. For statistical analyses, a two-tailed Student's *t*-test was used. $P < 0.05$ was regarded as statistically significant.

References

- Miller, G. Neuroscience. The dark side of glia. *Science* **308**, 778–781 (2005).
- Stellwagen, D. & Malenka, R. C. Synaptic scaling mediated by glial TNF- α . *Nature* **440**, 1054–1059 (2006).
- Barres, B. A. The mystery and magic of glia: a perspective on their roles in health and disease. *Neuron* **60**, 430–440 (2008).
- Campbell, K. & Götz, M. Radial glia: multi-purpose cells for vertebrate brain development. *Trends Neurosci.* **25**, 235–238 (2002).
- Alvarez-Buylla, A. & Lim, D. A. For the long run: maintaining germinal niches in the adult brain. *Neuron* **41**, 683–686 (2004).
- Tanaka, E.M. & Ferretti, P. Considering the evolution of regeneration in the central nervous system. *Nat. Rev. Neurosci.* **10**, 713–723 (2009).
- Matsugami, T. R. *et al.* Indispensability of the glutamate transporters GLAST and GLT1 to brain development. *Proc. Natl Acad. Sci. USA* **103**, 12161–12166 (2006).
- Harada, T. *et al.* Functions of the two glutamate transporters GLAST and GLT-1 in the retina. *Proc. Natl Acad. Sci. USA* **95**, 4663–4666 (1998).
- Harada, T. *et al.* The potential role of glutamate transporters in the pathogenesis of normal tension glaucoma. *J. Clin. Invest.* **117**, 1763–1770 (2007).
- Ooto, S. *et al.* Potential for neural regeneration after neurotoxic injury in the adult mammalian retina. *Proc. Natl Acad. Sci. USA* **101**, 13654–13659 (2004).
- Lamba, D., Karl, M. & Reh, T. Neural regeneration and cell replacement: a view from the eye. *Cell Stem Cell* **2**, 538–549 (2008).
- Harada, T. *et al.* Modification of glial-neuronal cell interactions prevents photoreceptor apoptosis during light-induced retinal degeneration. *Neuron* **26**, 533–541 (2000).
- Wahlin, K. J., Campochiaro, P. A., Zack, D. J. & Adler, R. Neurotrophic factors cause activation of intracellular signaling pathways in Müller cells and other cells of the inner retina, but not photoreceptors. *Invest. Ophthalmol. Vis. Sci.* **41**, 927–936 (2000).
- Bringmann, A. *et al.* Cellular signaling and factors involved in Müller cell gliosis: neuroprotective and detrimental effects. *Prog. Retin. Eye Res.* **28**, 423–451 (2009).
- Namekata, K. *et al.* Dock3 induces axonal outgrowth by stimulating membrane recruitment of the WAVE complex. *Proc. Natl Acad. Sci. USA* **107**, 7586–7591 (2010).
- Blum, R. & Konnerth, A. Neurotrophin-mediated rapid signaling in the central nervous system: mechanisms and functions. *Physiology* **20**, 70–78 (2005).
- Nikoletopoulou, V. *et al.* Neurotrophin receptors TrkA and TrkB cause neuronal death whereas TrkB does not. *Nature* **467**, 59–63 (2010).
- Grishanin, R. N. *et al.* Retinal TrkB receptors regulate neural development in the inner, but not outer, retina. *Mol. Cell Neurosci.* **38**, 431–443 (2008).
- Harada, T. *et al.* Microglia-Müller glia cell interactions control neurotrophic factor production during light-induced retinal degeneration. *J. Neurosci.* **22**, 9228–9236 (2002).
- Zhuo, L. *et al.* hGFAP-cre transgenic mice for manipulation of glial and neuronal function *in vivo*. *Genesis* **31**, 85–94 (2001).
- Malatesta, P. *et al.* Neuronal or glial progeny: regional differences in radial glia fate. *Neuron* **37**, 751–764 (2003).
- Soriano, P. Generalized lacZ expression with the ROSA26 Cre reporter strain. *Nat. Genet.* **21**, 70–71 (1999).
- Zhu, Y. *et al.* Inactivation of NF1 in CNS causes increased glial progenitor proliferation and optic glioma formation. *Development* **132**, 5577–5588 (2005).
- Eriksson, B., Bergqvist, I., Eriksson, M. & Holmberg, D. Functional expression of Cre recombinase in sub-regions of mouse CNS and retina. *FEBS Lett.* **479**, 106–110 (2000).
- Luikart, B. W. *et al.* TrkB has a cell-autonomous role in the establishment of hippocampal Schaffer collateral synapses. *J. Neurosci.* **25**, 3774–3786 (2005).
- Rocha, M., Martins, R. A. & Linden, R. Activation of NMDA receptors protects against glutamate neurotoxicity in the retina: evidence for the involvement of neurotrophins. *Brain Res.* **827**, 79–92 (1999).
- LaVail, M. M. *et al.* Multiple growth factors, cytokines, and neurotrophins rescue photoreceptors from the damaging effects of constant light. *Proc. Natl Acad. Sci. USA* **89**, 11249–11253 (1992).
- LaVail, M. M. *et al.* Sustained delivery of NT-3 from lens fiber cells in transgenic mice reveals specificity of neuroprotection in retinal degenerations. *J. Comp. Neurol.* **511**, 724–735 (2008).
- Wenzel, A., Grimm, C., Samardzija, M. & Remé, C. E. Molecular mechanisms of light-induced photoreceptor apoptosis and neuroprotection for retinal degeneration. *Prog. Retin. Eye Res.* **24**, 275–306 (2005).
- Yoshizawa, K. & Tsubura, A. Characteristics of *N*-methyl-*N*-nitrosourea-induced retinal degeneration in animals and application for the therapy of human retinitis pigmentosa. *Nippon Ganka Gakkai Zasshi* **109**, 327–337 (2005).
- Ju, B. G. *et al.* Activating the PARP-1 sensor component of the groucho/TLE1 corepressor complex mediates a CaMKII δ -dependent neurogenic gene activation pathway. *Cell* **119**, 815–829 (2004).
- Parras, C. M. *et al.* Mash1 specifies neurons and oligodendrocytes in the postnatal brain. *EMBO J.* **23**, 4495–4505 (2004).
- Tomita, K., Nakanishi, S., Guillemot, F. & Kageyama, R. Mash1 promotes neuronal differentiation in the retina. *Genes Cells* **1**, 765–774 (1996).
- Harada, T., Harada, C. & Parada, L. F. Molecular regulation of visual system development: more than meets the eye. *Genes Dev.* **21**, 367–378 (2007).
- Lipton, S. A. Retinal ganglion cells, glaucoma and neuroprotection. *Prog. Brain Res.* **131**, 712–718 (2001).
- Ohia, S. E., Opere, C. A. & LeDay, A. M. Pharmacological consequences of oxidative stress in ocular tissues. *Mutation Res.* **579**, 22–36 (2005).
- Harada, C. *et al.* Role of apoptosis signal-regulating kinase 1 in stress-induced neural cell apoptosis *in vivo*. *Am. J. Pathol.* **168**, 261–269 (2006).
- Harada, C. *et al.* ASK1 deficiency attenuates neural cell death in GLAST-deficient mice, a model of normal tension glaucoma. *Cell Death Differ.* **17**, 1751–1759 (2010).
- Johnson, E. C., Guo, Y., Cepurna, W.O. & Morrison, J. C. Neurotrophin roles in retinal ganglion cell survival: lessons from rat glaucoma models. *Exp. Eye Res.* **88**, 808–815 (2009).
- Morimoto, T. *et al.* Transcorneal electrical stimulation rescues axotomized retinal ganglion cells by activating endogenous retinal IGF-1 system. *Invest. Ophthalmol. Vis. Sci.* **46**, 2147–2155 (2005).
- Inomata, K. *et al.* Transcorneal electrical stimulation of retina to treat longstanding retinal artery occlusion. *Graefes Arch. Clin. Exp. Ophthalmol.* **245**, 1773–1780 (2007).
- Osakada, F. *et al.* Wnt signaling promotes regeneration in the retina of adult mammals. *J. Neurosci.* **27**, 4210–4219 (2007).
- Inestrosa, N. C. & Arenas, E. Emerging roles of Wnts in the adult nervous system. *Nat. Rev. Neurosci.* **11**, 77–86 (2010).
- Ernfors, P. & Bramham, C. R. The coupling of a trkB tyrosine residue to LTP. *Trends Neurosci.* **26**, 171–173 (2003).
- Rose, C. R. *et al.* Truncated TrkB-T1 mediates neurotrophin-evoked calcium signalling in glia cells. *Nature* **426**, 74–78 (2003).
- Faktorovich, E. G., Steinberg, R. H., Yasumura, D., Matthes, M. T. & LaVail, M. M. Basic fibroblast growth factor and local injury protect photoreceptors from light damage in the rat. *J. Neurosci.* **12**, 3554–3567 (1992).
- Yang, J. *et al.* Neuronal release of proBDNF. *Nat. Neurosci.* **12**, 113–115 (2009).
- Lee, R., Kerami, P., Teng, K. K. & Hempstead, B. L. Regulation of cell survival by secreted proneurotrophins. *Science* **294**, 1945–1948 (2001).
- Namekata, K., Harada, C., Kohyama, K., Matsumoto, Y. & Harada, T. Interleukin-1 stimulates glutamate uptake in glial cells by accelerating membrane trafficking of Na⁺/K⁺-ATPase via actin depolymerization. *Mol. Cell Biol.* **28**, 3273–3280 (2008).
- Guo, X. *et al.* Inhibition of glial cell activation ameliorates the severity of experimental autoimmune encephalomyelitis. *Neurosci. Res.* **59**, 457–466 (2007).

Acknowledgments

We thank A. Messing for providing GFAP-Cre mice, B. Eriksson for providing *c-kit*-Cre mice, R. Shimizu and M. Kasuya for technical assistance, and R. McKay for comments on the manuscript. This work was supported by the Ministry of Education, Culture, Sports, Science and Technology of Japan (C.H., X.G., K. Namekata, T.H.), the Ministry of Health, Labour and Welfare of Japan (K.T., T.H.), Japanese Retinitis Pigmentosa Society, the Japan Medical Association (T.H.), the National Institute of Neurological Disorders and Stroke, the American Cancer Society, and the Department of Defense (L.F.P.).

Author contributions

C.H., L.F.P. and T.H. designed the study and wrote the paper. K. Namekata and K.T. contributed to the study design. C.H., X.G., K. Namekata, A.K., K. Nakamura and T.H. conducted the experiments. All authors interpreted the data.

Additional information

Supplementary Information accompanies this paper at <http://www.nature.com/naturecommunications>

Competing financial interests: The authors declare no competing financial interests.

Reprints and permission information is available online at <http://npg.nature.com/reprintsandpermissions/>

How to cite this article: Harada, C. *et al.* Glia- and neuron-specific functions of TrkB signalling during retinal degeneration and regeneration. *Nat. Commun.* 2:189 doi: 10.1038/ncomms1190 (2011).

License: This work is licensed under a Creative Commons Attribution-NonCommercial-Share Alike 3.0 Unported License. To view a copy of this license, visit <http://creativecommons.org/licenses/by-nc-sa/3.0/>

Supplementary information:

Glia- and neuron-specific functions of TrkB signaling during retinal degeneration and regeneration

Chikako Harada,^{1,2} Xiaoli Guo,¹ Kazuhiko Namekata,¹ Atsuko Kimura,¹ Kazuaki Nakamura,¹ Kohichi Tanaka,³ Luis F. Parada,² and Takayuki Harada^{1,2}

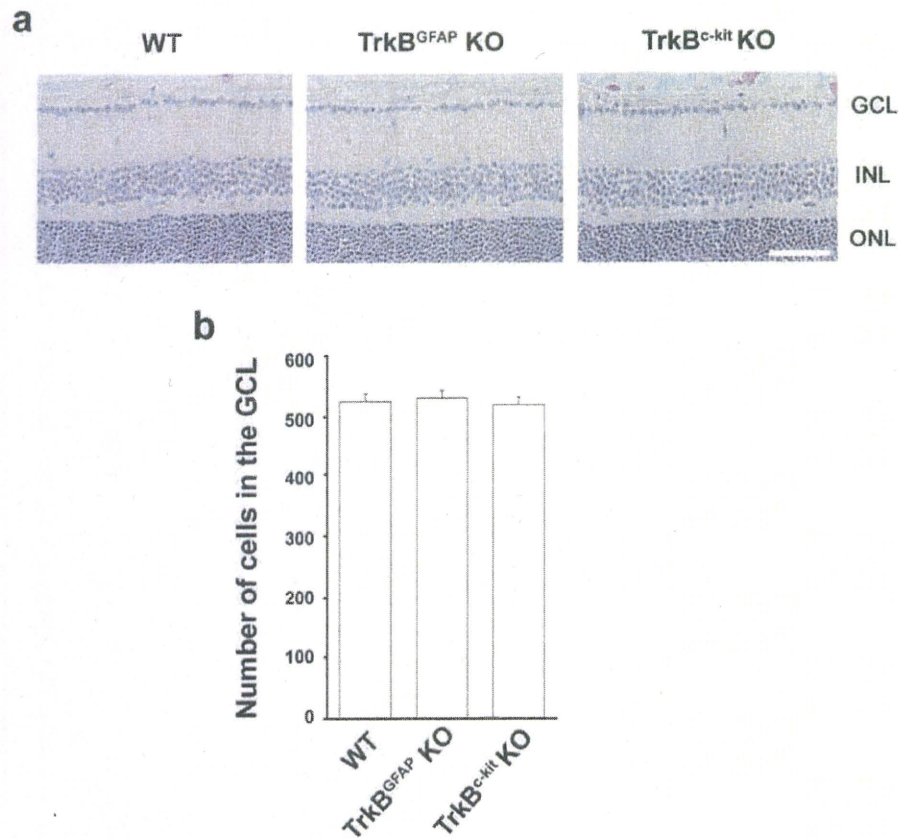
¹Department of Molecular Neurobiology, Tokyo Metropolitan Institute for Neuroscience, Fuchu, Tokyo 183-8526, Japan

²Department of Developmental Biology and Kent Waldrep Foundation Center for Basic Research on Nerve Growth and Regeneration, University of Texas Southwestern Medical Center, Dallas, TX 75390-9133, USA

³ Laboratory of Molecular Neuroscience, School of Biomedical Science and Medical Research Institute, Tokyo Medical and Dental University, Tokyo 113-8510, Japan

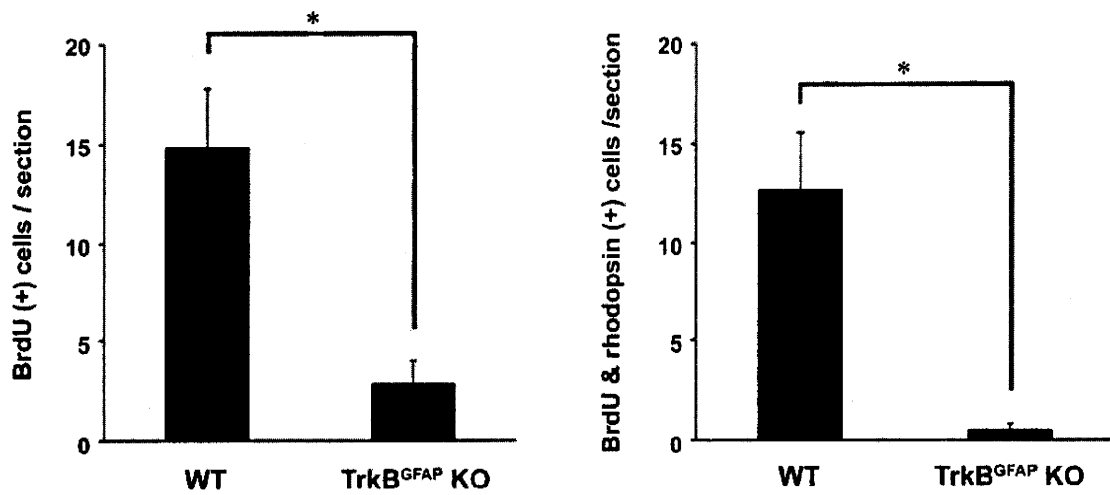
Supplementary Figures S1-S2

Supplementary Table S1



Supplementary Figure S1: Histological analysis of the adult retina in TrkB^{GFAP} KO and TrkB^{c-kit} KO mice.

(a) Retinal sections stained with hematoxylin and eosin in WT, TrkB^{GFAP} KO and TrkB^{c-kit} KO mice. Scale bar = 50 μ m. GCL, ganglion cell layer; INL, inner nuclear layer; ONL, outer nuclear layer. (b) Quantitative analysis of cell numbers in the GCL. Data are shown as the mean \pm s.e.m. ($n = 6$). □ □



Supplementary Figure S2: Quantitative analysis of the proliferating cells after BDNF treatment in MNU-induced model of photoreceptor degeneration.

Retinal sections were stained with antibodies against BrdU and rhodopsin, and the number of immunopositive cells were counted in WT and TrkB^{GFAP} KO mice. Data are shown as the mean \pm s.e.m. ($n = 6$). * $P < 0.01$.

Supplementary Table S1: PCR primers used in this study.

Gene	Primer sequence	
	Forward	Reverse
NGF	5'-CGACTCCAAACACTGGA ACTCA-3'	5'-GCCTGCTTCTCACTGTGTGCA-3'
BDNF	5'-ATGCCGCAAACATGTCTATGAG-3'	5'-TGACCCACTCGCTAATACTGTCA-3'
NT-3	5'-GTTCCAGCCAATGATTGCAA-3'	5'-GGGCGAATTGTAGCGTCTCT-3'
NT-4	5'-GAGGCACTGGCTCTCAGAATG-3'	5'-CGAATCCAGCGCCAGC-3'
bFGF	5'-CACCAGGCCACTTCAAGGA-3'	5'-GATGGATGCGCAGGAAGAA-3'
CNTF	5'-GGTGACTTCCATCAGGCAATACA-3'	5'-CTGTTCCAGAAGCGCCATTAAAC-3'
GDNF	5'-GGCTACCTTGTCACCTGTTAGC-3'	5'-GGCTACTTTGTCACTTGTTAGC-3'
CaMKII α	5'-TTTGCCCTCTTCAGGCTTTA-3'	5'-CTTCTCCCACACGIGAACAA-3'
CaMKII β	5'-TGACCTGGGCCTAGAGAAGA-3'	5'-TCTCTGGCCTACCTGGAAGA-3'
CaMKII δ	5'-CCAAAGACCATGCAGTCAGA-3'	5'-ATTCTGCCACTTCCCATCAC-3'
CaMKII γ	5'-ACCGGTCCAGTTAGCGTAGA-3'	5'-CACACTTCTGCAGCACCAAT-3'
Hes1	5'-CGGTCTACACCAGCAACAGT-3'	5'-AGCCACTGGAAGGTGACACT-3'
Mash1	5'-TCTCCGGTCTCGTCTACTC-3'	5'-GTCCAGCAGCTCTTGTTCCCT-3'
GAPDH	5'-TGCACCACCAACTGCTTAG-3'	5'-TGCACCACCAACTGCTTAG-3'

NGF, nerve growth factor; BDNF, brain-derived neurotrophic factor; NT-3, neurotrophin-3; NT-4, neurotrophin-4; bFGF, basic fibroblast growth factor; CNTF, ciliary neurotrophic factor; GDNF, glial cell line-derived neurotrophic factor; GAPDH, glyceraldehyde-3-phosphate dehydrogenase.

